References

Bamshad MJ, Ng SB, Bigham AW, Tabor HK, Emond MJ, Nickerson DA, Shendure J. 2011. Exome sequencing as a tool for Mendelian disease gene discovery. Nat Rev Genet 12:745–755.

Barcia G, Fleming MR, Deligniere A, Gazula VR, Brown MR, Langouet M, Chen H, Kronengold J, Abhyankar A, Cilio R, Nitschke P, Kaminska A, et al. 2012. *De novo* gain-of-function *KCNT1* channel mutations cause malignant migrating partial seizures of infancy. Nat Genet 44:1255–1259.

Claes L, Del-Favero J, Ceulemans B, Lagae L, Van Broeckhoven C, De Jonghe P. 2001. De novo mutations in the sodium-channel gene *SCN1A* cause severe myoclonic epilepsy of infancy. Am J Hum Genet 68:1327–32.

DePristo MA, Banks E, Poplin R, Garimella KV, Maguire JR, Hartl C, Philippakis AA, del Angel G, Rivas MA, Hanna M, McKenna A, Fennell TJ, et al. 2011. A framework for variation discovery and genotyping using next-generation DNA sequencing data. Nat Genet 43:491–498.

Freeze HH. 2006. Genetic defects in the human glycome. Nat Rev Genet 7:537–551.

Freeze HH. 2013. Understanding human glycosylation disorders: biochemistry leads the charge. J Biol Chem 288:6936–6945.

Freeze HH, Eklund EA, Ng BG, Patterson MC. 2012. Neurology of inherited glycosylation disorders. Lancet Neurol 11:453–466.

Goreta SS, Dabelic S, Dumic J. 2012. Insights into complexity of congenital disorders of glycosylation. Biochem Med (Zagreb) 22:156–170.

Hiraoka S, Furuichi T, Nishimura G, Shibata S, Yanagishita M, Rimoin DL, Superti-Furga A, Nikkels PG, Ogawa M, Katsuyama K, Toyoda H, Kinoshita-Toyoda A, et al. 2007. Nucleotide-sugar transporter SLC35D1 is critical to chondroitin sulfate synthesis in cartilage and skeletal development in mouse and human. Nat Med 13:1363–1367.

Holland KD, Hallinan BE. 2010. What causes epileptic encephalopathy in infancy?: the answer may lie in our genes. Neurology 75:1132–1133.

Hu H, Eggers K, Chen W, Garshasbi M, Motazacker MM, Wrogemann K, Kahrizi K, Tzschach A, Hosseini M, Bahman I, Hucho T, Mühlenhoff M, et al. 2011. *ST3GAL3* mutations impair the development of higher cognitive functions. Am J Hum Genet 89:407–414.

Ishida N, Miura N, Yoshioka S, Kawakita M. 1996. Molecular cloning and characterization of a novel isoform of the human UDP-galactose transporter, and of related complementary DNAs belonging to the nucleotide-sugar transporter gene family. J Biochem 120:1074–1078.

Jaeken J. 2003. Komrower Lecture. Congenital disorders of glycosylation (CDG): it's all in it! J Inherit Metab Dis 26:99–118.

Jaeken J, Matthijs G. 2007. Congenital disorders of glycosylation: a rapidly expanding disease family. Annu Rev Genomics Hum Genet 8:261–278.

Kabuss R, Ashikov A, Oelmann S, Gerardy-Schahn R, Bakker H. 2005. Endoplasmic reticulum retention of the large splice variant of the UDP-galactose transporter is caused by a dilysine motif. Glycobiology 15:905–911.

Kalscheuer VM, Tao J, Donnelly A, Hollway G, Schwinger E, Kubart S, Menzel C, Hoeltzenbein M, Tommerup N, Eyre H, Harbord M, Haan E, Sutherland GR, Ropers HH, Gécz J. 2003. Disruption of the serine/threonine kinase 9 gene causes severe X-linked infantile spasms and mental retardation. Am J Hum Genet 72:1401–1411.

Kato M, Saitoh S, Kamei A, Shiraishi H, Ueda Y, Akasaka M, Tohyama J, Akasaka N, Hayasaka K. 2007. A longer polyalanine expansion mutation in the *ARX* gene causes early infantile epileptic encephalopathy with suppression-burst pattern (Ohtahara syndrome). Am J Hum Genet 81:361–366.

Kondo Y, Saitsu H, Miyamoto T, Nishiyama K, Tsurusaki Y, Doi H, Miyake N, Ryoo NK, Kim JH, Yu YS, and others. 2012. A family of oculofaciocardiodental syndrome (OFCD) with a novel BCOR mutation and genomic rearrangements involving NHS. J Hum Genet 57:197–201.

Kurian MA, Meyer E, Vassallo G, Morgan NV, Prakash N, Pasha S, Hai NA, Shuib S, Rahman F, Wassmer E, Cross JH, O'Callaghan FJ, et al. 2010. Phospholipase C beta 1 deficiency is associated with early-onset epileptic encephalopathy. Brain 133:2964–2970.

Liu L, Xu YX, Hirschberg CB. 2010. The role of nucleotide sugar transporters in development of eukaryotes. Semin Cell Dev Biol 21:600–608.

Lubke T, Marquardt T, Etzioni A, Hartmann E, von Figura K, Korner C. 2001. Complementation cloning identifies CDG-IIc, a new type of congenital disorders of glycosylation, as a GDP-fucose transporter deficiency. Nat Genet 28:73–76.

Luhn K, Wild MK, Eckhardt M, Gerardy-Schahn R, Vestweber D. 2001. The gene defective in leukocyte adhesion deficiency II encodes a putative GDP-fucose transporter. Nat Genet 28:69–72.

Martinez-Duncker I, Dupre T, Piller V, Piller F, Candelier JJ, Trichet C, Tchernia G, Oriol R, Mollicone R. 2005. Genetic complementation reveals a novel human congenital disorder of glycosylation of type II, due to inactivation of the Golgi CMP-sialic acid transporter. Blood 105:2671–2676.

Mills PB, Surtees RA, Champion MP, Beesley CE, Dalton N, Scambler PJ, Heales SJ, Briddon A, Scheimberg I, Hoffmann GF, Zschocke J, Clayton PT. 2005. Neonatal epileptic encephalopathy caused by mutations in the *PNPO* gene encoding pyridox(am)ine 5′-phosphate oxidase. Hum Mol Genet 14:1077–1086.

Miura N, Ishida N, Hoshino M, Yamauchi M, Hara T, Ayusawa D, Kawakita M. 1996. Human UDP-galactose translocator: molecular cloning of a complementary DNA that complements the genetic defect of a mutant cell line deficient in UDP-galactose translocator. J Biochem 120:236–241.

Molinari F, Raas-Rothschild A, Rio M, Fiermonte G, Encha-Razavi F, Palmieri L, Palmieri F, Ben-Neriah Z, Kadhom N, Vekemans M, Attie-Bitach T, Munnich A, Rustin P, Colleaux L. 2005. Impaired mitochondrial glutamate transport in autosomal recessive neonatal myoclonic epilepsy. Am J Hum Genet 76:334–339.

Muntoni F. 2004. Journey into muscular dystrophies caused by abnormal glycosylation. Acta Myol 23:79–84.

Ng BG, Buckingham KJ, Raymond K, Kircher M, Turner EH, He M, Smith JD, Eroshkin A, Szybowska M, Losfeld ME, Chong JX, Kozenko M, et al. 2013. Mosaicism of the UDP-galactose transporter *SLC35A2* causes a congenital disorder of glycosylation. Am J Hum Genet 92:632–636.

Oelmann S, Stanley P, Gerardy-Schahn R. 2001. Point mutations identified in Lec8 Chinese hamster ovary glycosylation mutants that inactivate both the UDP-galactose and CMP-sialic acid transporters. J Biol Chem 276:26291–26300.

Okanishi T, Saito Y, Yuasa I, Miura M, Nagata I, Maegaki Y, Ohno K. 2008. Cutis laxa with frontoparietal cortical malformation: a novel type of congenital disorder of glycosylation. Eur J Paediatr Neurol 12:262–265.

Saitsu H, Kato M, Koide A, Goto T, Fujita T, Nishiyama K, Tsurusaki Y, Doi H, Miyake N, Hayasaka K, Matsumoto N. 2012a. Whole exome sequencing identifies *KCNQ2* mutations in Ohtahara syndrome. Ann Neurol 72:298–300.

Saitsu H, Kato M, Mizuguchi T, Hamada K, Osaka H, Tohyama J, Uruno K, Kumada S, Nishiyama K, Nishimura A, Okada A, Yoshimura Y, et al. 2008. *De novo* mutations in the gene encoding STXBP1 (MUNC18-1) cause early infantile epileptic encephalopathy. Nat Genet 40:782–788.

Saitsu H, Kato M, Okada I, Orii KE, Higuchi T, Hoshino H, Kubota M, Arai H, Tagawa T, Kimura S, Sudo A, Miyama S, et al. 2010. *STXBP1* mutations in early infantile epileptic encephalopathy with suppression-burst pattern. Epilepsia 51:2397–2405.

Saitsu H, Kato M, Osaka H, Moriyama N, Horita H, Nishiyama K, Yoneda Y, Kondo Y, Tsurusaki Y, Doi H, Miyake N, Hayasaka K, Matsumoto N. 2012b. *CASK* aberrations in male patients with Ohtahara syndrome and cerebellar hypoplasia. Epilepsia 53:1441–1449.

Saitsu H, Nishimura T, Muramatsu K, Kodera H, Kumada S, Sugai K, Kasai-Yoshida E, Sawaura N, Nishida H, Hoshino A, Ryujin F, Yoshioka S, et al. 2013. *De novo* mutations in the autophagy gene *WDR45* cause static encephalopathy of childhood with neurodegeneration in adulthood. Nat Genet 45:445–449.

Shen J, Gilmore EC, Marshall CA, Haddadin M, Reynolds JJ, Eyaid W, Bodell A, Barry B, Gleason D, Allen K, Ganesh VS, Chang BS, et al. 2010. Mutations in *PNKP* cause microcephaly, seizures and defects in DNA repair. Nat Genet 42: 245–249.

Stromme P, Mangelsdorf ME, Shaw MA, Lower KM, Lewis SM, Bruyere H, Lutcherath V, Gedeon AK, Wallace RH, Scheffer IE, Turner G, Partington M, et al. 2002. Mutations in the human ortholog of Aristaless cause X-linked mental retardation and epilepsy. Nat Genet 30:441–445.

Wada Y, Azadi P, Costello CE, Dell A, Dwek RA, Geyer H, Geyer R, Kakehi K, Karlsson NG, Kato K, Kawasaki N, Khoo KH, et al. 2007. Comparison of the methods for profiling glycoprotein glycans–HUPO Human Disease Glycomics/Proteome Initiative multi-institutional study. Glycobiology 17:411–422.

Wada Y, Kadoya M, Okamoto N. 2012. Mass spectrometry of apolipoprotein C-III, a simple analytical method for mucin-type O-glycosylation and its application to an autosomal recessive cutis laxa type-2 (ARCL2) patient. Glycobiology 22:1140–1144.

Wang K, Li M, Hakonarson H. 2010. ANNOVAR: functional annotation of genetic variants from high-throughput sequencing data. Nucleic Acids Res 38:e164.

Weckhuysen S, Mandelstam S, Suls A, Audenaert D, Deconinck T, Claes LR, Deprez L, Smets K, Hristova D, Yordanova I, Jordanova A, Ceulemans B, et al. 2012. *KCNQ2* encephalopathy: emerging phenotype of a neonatal epileptic encephalopathy. Ann Neurol 71:15–25.

Wopereis S, Lefeber DJ, Morava E, Wevers RA. 2006. Mechanisms in protein O-glycan biosynthesis and clinical and molecular aspects of protein O-glycan biosynthesis defects: a review. Clin Chem 52:574–600.

Yoshioka S, Sun-Wada GH, Ishida N, Kawakita M. 1997. Expression of the human UDP-galactose transporter in the Golgi membranes of murine Had-1 cells that lack the endogenous transporter. J Biochem 122:691–695.

Neurogenetics (2013) 14:225–232
DOI 10.1007/s10048-013-0375-8

ORIGINAL ARTICLE

Diagnostic utility of whole exome sequencing in patients showing cerebellar and/or vermis atrophy in childhood

Chihiro Ohba · Hitoshi Osaka · Mizue Iai · Sumimasa Yamashita · Yume Suzuki · Noriko Aida · Nobuyuki Shimozawa · Ayumi Takamura · Hiroshi Doi · Atsuko Tomita-Katsumoto · Kiyomi Nishiyama · Yoshinori Tsurusaki · Mitsuko Nakashima · Noriko Miyake · Yoshikatsu Eto · Fumiaki Tanaka · Naomichi Matsumoto · Hirotomo Saitsu

Received: 9 July 2013 / Accepted: 18 September 2013 / Published online: 4 October 2013

Abstract Cerebellar and/or vermis atrophy is recognized in various types of childhood disorders with clinical and genetic heterogeneity. Although careful evaluation of clinical features and neuroimaging can lead to correct diagnosis of disorders, their diagnosis is sometimes difficult because clinical features can overlap with each other. In this study, we performed family-based whole exome sequencing of 23 families including 25 patients with cerebellar and/or vermis atrophy in childhood, who were unable to be diagnosed solely by clinical examination. Pathological mutations of seven genes were found in ten patients from nine families (9/23, 39.1 %): compound heterozygous mutations in *FOLR1*, *C5orf42*, *POLG*, *TPP1*, *PEX16*, and de novo mutations in *CACNA1A*, and *ITPR1*. Patient 1A with *FOLR1* mutations showed extremely low concentration of 5-methyltetrahydrofolate in the cerebrospinal fluid and serum, and Patient 6 with *TPP1* mutations demonstrated markedly lowered tripeptidyl peptidase 1 activity in leukocytes. Furthermore, Patient 8 with *PEX16* mutations presented a mild increase of very long chain fatty acids in the serum as supportive data for genetic diagnosis. The main clinical features of these ten patients were nonspecific and mixed, and included developmental delay, intellectual disability, ataxia, hypotonia, and epilepsy. Brain MRI revealed both cerebellar and vermis atrophy in eight patients (8/10, 80 %), vermis atrophy/hypoplasia in two patients (2/10, 20 %), and brainstem atrophy in one patient (1/10, 10 %).

Electronic supplementary material The online version of this article (doi:10.1007/s10048-013-0375-8) contains supplementary material, which is available to authorized users.

C. Ohba · K. Nishiyama · Y. Tsurusaki · M. Nakashima · N. Miyake · N. Matsumoto (✉) · H. Saitsu (✉)
Department of Human Genetics, Graduate School of Medicine, Yokohama City University, 3-9 FukuuraKanazawa-ku Yokohama 236-0004, Japan
e-mail: naomat@yokohama-cu.ac.jp
e-mail: hsaitsu@yokohama-cu.ac.jp

C. Ohba
e-mail: t116017g@yokohama-cu.ac.jp

K. Nishiyama
e-mail: kiyomim@yokohama-cu.ac.jp

Y. Tsurusaki
e-mail: tsurusak@yokohama-cu.ac.jp

M. Nakashima
e-mail: mnakashi@yokohama-cu.ac.jp

N. Miyake
e-mail: nmiyake@yokohama-cu.ac.jp

C. Ohba · Y. Suzuki · H. Doi · A. Tomita-Katsumoto · F. Tanaka
Department of Clinical Neurology and Stroke Medicine, Yokohama City University, Yokohama 236-0004, Japan

Y. Suzuki
e-mail: yume@med.yokohama-cu.ac.jp

H. Doi
e-mail: doi@rkd.d-bs.com

A. Tomita-Katsumoto
e-mail: chiwawan-atsuko@hotmail.co.jp

F. Tanaka
e-mail: ftanaka@yokohama-cu.ac.jp

H. Osaka · M. Iai · S. Yamashita
Division of Neurology, Kanagawa Children's Medical Center, Clinical Research Institute, Yokohama 232-0066, Japan

H. Osaka
e-mail: hosaka@kcmc.jp

Our data clearly demonstrate the utility of whole exome sequencing for genetic diagnosis of childhood cerebellar and/or vermis atrophy.

Keywords Cerebellar and/or vermis atrophy · Whole exome sequencing · De novo mutation · Compound heterozygous mutation

Introduction

Cerebellar atrophy in childhood can be classified into three types: hereditary cerebellar atrophy, postnatally acquired cerebellar atrophy, and unilateral cerebellar atrophy [1]. The number of differential diagnoses for hereditary cerebellar atrophy in childhood exceeds 70 diseases, the clinical findings of which often overlap with each other [1]. For example, ataxia was recognized as one of the main symptoms in 36 diseases, intellectual disability in 14 diseases, and epilepsy in 20 diseases [1].

In a review of 402 patients with cerebellar abnormality on magnetic resonance imaging (MRI), 66 patients showed posterior fossa malformation including Joubert syndrome [2]. Among 300 patients with cerebellar atrophy, in whom nongenetic etiologies were excluded, clinical diagnosis was established in 142 patients (47 %), and consisted of mitochondrial disorders (37 patients), neuronal ceroid lipofuscinosis (25 patients), ataxia telangiectasia (14 patients), and GM2 gangliosidosis (10 patients) [2]. The estimated prevalence of these disorders is rare, with reports of only 9.2 per 100,000 people affected with mitochondrial disorders in northeast England [3], 1.2 per 1,000,000 with neuronal ceroid lipofuscinosis in Italy [4], and 0.4 per 100,000 with ataxia telangiectasia in southeast Norway [5]. Therefore, clinical diagnosis of disorders with cerebellar abnormality is often difficult as many rare disorders with overlapping clinical features are included in this condition.

The genetic diagnosis of cerebellar and/or vermis atrophy is more challenging. Causative mutations for cerebellar atrophy and ataxia disorders have been found in more than 150 genes [1, 2, 6–8]. Joubert syndrome, which shows vermis atrophy/hypoplasia, is also genetically heterogeneous as mutations in 21 genes have been reported [7]. Whole exome sequencing (WES), which employs the targeted capture of protein encoding exons and massively parallel DNA sequencing, has enabled the comprehensive examination of mutations in more than 90 % of exons [9]. In addition, de novo or recessive mutations can be systemically identified by family-based exome sequencing using trios of a patient and his/her parents [10], suggesting that WES is useful for genetic diagnosis in heterogeneous genetic disorders. Indeed, family-based WES successfully detected disease-causing mutations in 16 of 100 patients with severe intellectual disability, which were both clinically and genetically heterogeneous [11].

In this study, we performed family-based WES in 23 families including 25 patients who showed cerebellar and/or vermis atrophy in childhood on a brain MRI. We successfully identified disease-causing mutations in nine families (9/23, 39.1 %).

Patients and methods

Patients

We analyzed 23 families including 25 patients with various degrees of cerebellar and/or vermis atrophy on brain MRI, and their unaffected parents and siblings (if available). All patients were sporadic, except for two who each had two affected siblings. Clinical examination failed to provide a clear diagnosis for each of the patients included in this study. Both static malformations and progressive cerebellar atrophy were included. Serum levels of lactic acid and pyruvate fell within the normal range for all patients. α-fetoprotein, total-cholesterol, and immunoglobulin levels were measured to exclude ataxia telangiectasia. Serum levels of albumin and tocopherol were examined in 23 of 25 patients, excluding early-onset ataxia with oculomotor apraxia and hypoalbuminemia, and ataxia with isolated vitamin E deficiency, respectively (Supplementary Table 1). Genomic DNA was isolated from peripheral blood leukocytes using QuickGene 610 L

M. Iai
e-mail: miai@kcmc.jp

S. Yamashita
e-mail: syamashita@kcmc.jp

N. Aida
Division of Radiology, Kanagawa Children's Medical Center, Clinical Research Institute, Yokohama 232-0066, Japan
e-mail: naida@kcmc.jp

N. Shimozawa
Division of Genomics Research, Life Science Research Center, Gifu University, Gifu 501-1193, Japan
e-mail: nshim@gifu-u.ac.jp

A. Takamura · Y. Eto
Department of Genetics and Genome Science, Tokyo Jikei University School of Medicine, Tokyo 105-8461, Japan

A. Takamura
e-mail: ayumi.takamura@mt.strins.or.jp

Y. Eto
e-mail: yosh@sepia.ocn.ne.jp

A. Takamura · Y. Eto
Advanced Clinical Research Center, Institute of Neurological Disorders, Kawasaki 215-0026, Japan

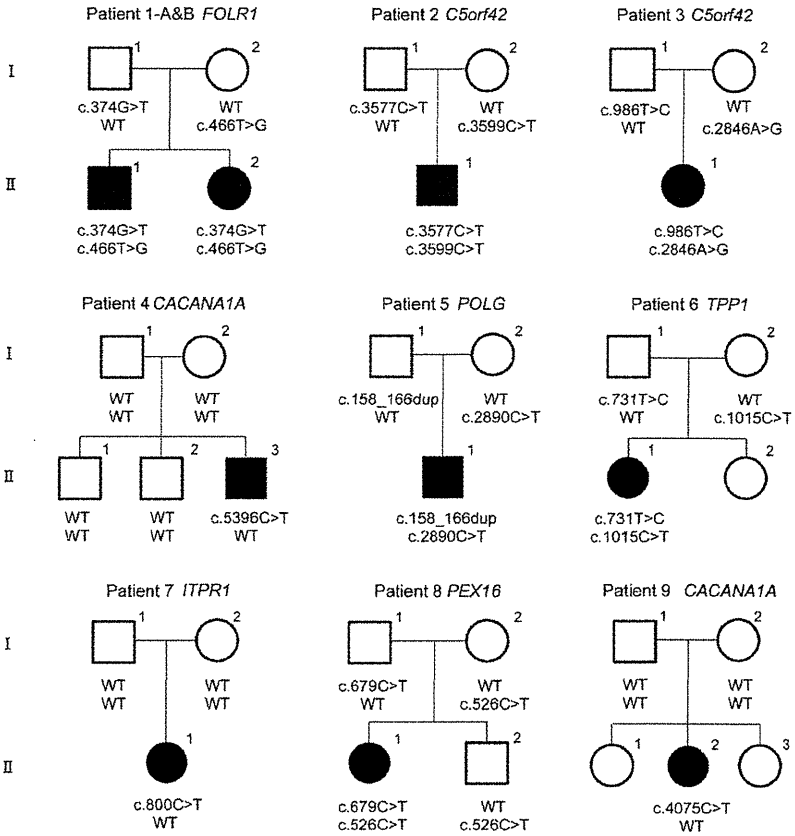

Fig. 1 Pedigrees of nine kindreds with cerebellar atrophy in childhood. Causative mutations were identified in seven genes. The segregation of each mutation is shown

(Wako, Osaka, Japan). The Institutional Review Board of Yokohama City University School of Medicine approved the experimental protocols. Informed consent was obtained for all individuals included in this study in agreement with the requirements of Japanese regulations.

Whole exome sequencing

Genomic DNA was captured using the SureSelect Human All Exon v4 Kit (51 Mb; Agilent Technologies, Santa Clara, CA, USA) and sequenced on an Illumina HiSeq2000 (Illumina, San Diego, CA, USA) with 101 bp paired-end reads. Four samples were run in one lane of the flow cell. Exome data processing, variant calling, and variant annotation were performed as previously described [12].

Results

Family-based WES was performed in 23 families including 25 patients and their unaffected parents and siblings. The average read depth of the protein-coding regions of RefSeq genes was 124.50 (range across all samples, 81.85–185.67), such that 94.3 % of targeted coding sequences was covered by 10 reads or more. We filtered out common single nucleotide polymorphisms (SNPs) that met the following two criteria: variants showing minor allele frequencies ≥1% in dbSNP 135 and variants found in more than two of our in-house 406 control exomes. Protein-altering and splicing-affecting variants were considered for downstream analysis. Mutations in previously reported causative genes for cerebellar atrophy were examined with particular attention (Supplementary Table 1).

All genes were surveyed for de novo mutations and compound heterozygous or homozygous mutations in each family. We identified pathological mutations in seven genes within nine families (9/23, 39.1%): compound heterozygous *FOLR1* mutations in patients 1A and 1B (siblings) [c.374G>T (p.R125L) and c.466T>G (p.W156G)]; a de novo *CACNA1A* mutation in patients 4 and 9 [c.5396C>T (p.S1799L) and c.4075C>T (p.R1359W)], respectively; compound heterozygous *C5orf42* mutations in patients 2 and 3 [c.3577C>T(p.R1193C) and c.3599C>T (p.A1200V) in patient 2, c.986T>C (p.L329P) and c.2846A>G (p.Y949C) in patient 3]; compound heterozygous *POLG* mutations in patient 5 [c.158_166dup (p.Q53_Q55dup) and c.2890C>T (p.R964C)]; compound heterozygous *TPP1* mutations in patient 6 [c.731T>C (p.M244T) and c.1015C>T (p.R339W)]; a de novo *ITPR1* mutation in patient 7 [c.800C>T (p.T267M)]; and compound heterozygous *PEX16* mutations in patient 8 [c.679C>T (p.R227W) and c.526C>T (p.R176*)] (Fig. 1 and Table 1). These mutations were confirmed by Sanger

Table 1 Clinical features of patients

Patient number	1-A	1-B	2	3	4	5	6	7	8	9
Age (years), gender	17 years, male	14 years, female	5 years, male	2 years, female	8 years, male	8 years, male	5 years, female	6 years, female	9 years, female	20 years, female
Gene mutated	*FOLR1*	*FOLR1*	*C5orf42*	*C5orf42*	*CACNA1A*	*POLG*	*TPP1*	*ITPR1*	*PEX16*	*CACNA1A*
Known disease(s) caused by mutations	Neurodegeneration from cerebral folate transport deficiency	Neurodegeneration from cerebral folate transport deficiency	Joubert syndrome	Joubert syndrome	SCA6, Episodic ataxia type 2, FHM1	mtDNA depletion syndrome, Mitochondrial recessive ataxia syndrome, PEO	Neuronal ceroid lipofuscinosis type2, autosomal recessive spinocerebellar ataxia type 7	SCA15, SCA29	Zellweger syndrome	SCA6, Episodic ataxia type 2, FHM1
Mutations (number of control exomes harboring the mutation/total control exomes)	c.374G>T p.R125L (0/406) c.466T>G p.W156G (0/406)	c.374G>T p.R125L (0/406) c.466T>G p.W156G (0/406)	c.3577C>T p.R1193C (0/406) c.3599C>T p.A1200V (0/406)	c.986T>C p.L329P (0/406) c.2846A>G p.Y949C (0/406)	c.5396C>T p.S1799L (0/406)	c.158_166dup p.Q53_Q55dup (0/406) c.2890C>T[a] p.R964C (2/406)	c.731T>C p.M244T (0/406) c.1015C>T p.R339W (0/406)	c.800C>T p.T267-M (0/406)	c.679C>T p.R227W (0/406) c.526C>T[a] p.R176* (0/406)	c.4075C>T p.-R1359-W (0/406)
Inheritance	Compound heterozygous	Compound heterozygous	Compound heterozygous	Compound heterozygous	De novo	Compound heterozygous	Compound heterozygous	De novo	Compound heterozygous	De novo
Initial symptom	Ataxic gait	Ataxic gait	Developmental delay	Hypotonia	Developmental delay	Hypotonia	Epilepsy	Hypotonia/nystagmus	Ataxic gait	Epilepsy
Age at onset	1 years	2 years	9 months	1 years	9 months	6 months	3 years	4 months	1 years	3 months
Ataxia	+	+	−	+	+	+	+	+	+	+
Dysmetria	−	−	−	−	+	−	+	−	+	+
Oculomotor apraxia	−	−	+	+	+	−	−	−	+	+
Intention tremor	+	+	−	−	+	−	−	+	+	+
Other	Slurred speech	Slurred speech					Slurred speech	Nystagmus/slurred speech	Slurred speech	Slurred speech
Developmental delay	+	+	+	+	+	+	+	+	+	+
Intellectual disability	+	+	+	+	+	+	+	+	−	+
Speech ability	Three-word sentences	Three-word sentences	Two-word sentences	Two-word sentences	Few words	N.D.	Three-word sentences	Three-word sentences	Few words	Few words
Muscle tone	Mild hypotonia/spastic lower limbs	Mild hypotonia	Hypotonia	Hypotonia	Hypotonia	Hypotonia	−	Hypotonia	Hypotonia	Hypotonia
Pyramidal sign	+	−	−	−	−	−	−	−	−	+ (DTR↑)
Extrapyramidal sign	−	−	−	−	−	−	−	−	−	−
Peripheral neuropathy	−	N.D.	N.D	N.D.	−	N.D.	N.D.	N.D.	−	−
Epileptic seizure	+	+	−	−	+	−	+	−	−	+
Complication	Low IgG			Aortic coarctation					Pigmentary retinal	

Table 1 (continued)

Patient number	1-A	1-B	2	3	4	5	6	7	8	9
MRI									degeneration	
Cerebellar atrophy/ hypoplasia	+	+	Vermis atrophy	Vermis hypoplasia	+	+	+	+	+ (mild)	+
Brainstem atrophy	+ (mild)	–	–	–	–	–	–	–	–	–
Other	Cerebral WM atrophy, Calcification at subcortical WM	Calcification at basal ganglia and subcortical WM	Molar tooth sign							

WM white matter, *PEO* progressive external ophthalmoplegia, *FHM1* familial hemiplegic migraine type1, *mtDNA* mitochondrial DNA, *DTR* deep tendon reflex, *N.D.* not detected

[a] This mutation has been previously reported as disease-causing

sequencing. Five of 15 mutations were registered in dbSNP (http://www.ncbi.nlm.nih.gov/projects/SNP/) as rare variants (Supplementary Table 2). None of the mutations were present in the 6,500 exomes sequenced by the National Heart, Lung, and Blood Institute exome project or our 406 in-house control exomes, except for c.2890C>T in *POLG*, which was found in 2 of 406 control exomes (Table 1, and Supplementary Table 2). Two mutations (c.2890C>T in *POLG* and c.526C>T in *PEX16*) have been reported as disease-causing mutations [13, 14]. All of the single nucleotide substitutions (SNVs) occurred at evolutionally conserved amino acids (as shown by high PhyloP score), and Sorting Intolerant From Tolerant (SIFT), Polyphen2, and Mutation Taster predicted that all the SNVs would be highly damaging to the protein structure (Supplementary Table 2), supporting pathogenicity of the mutations.

Clinical features of the ten patients are summarized in Table 1 (see also supplementary Case report). All patients exhibited motor developmental delay (10/10, 100%), and nine patients had an intellectual disability (9/10, 90%). All patients showed cerebellar signs (10/10, 100%) such as ataxia of the limbs and trunk, oculomotor apraxia, dysmetria, intention tremor, slurred speech and nystagmus. Hypotonia and epileptic seizures were observed in nine and five patients, respectively (9/10, 90%; 5/10, 50%). Patient 1B with compound heterozygous *FOLR1* mutations, which cause neurodegeneration from cerebral folate transport deficiency [15, 16], showed an extremely low concentration of 5-methyltetrahydrofolate (5-MTHF) in the cerebrospinal fluid and serum (0.0 nmol/l and 5.0 nmol/l). In patient 6 with compound heterozygous *TPP1* mutations, markedly low activity of tripeptidyl peptidase 1 was observed: 5.44 nmol/mg/h in leukocytes and 0.092 pmol/punch/h in dried blood spot (Supplementary Table 3) [17, 18]. Patient 8 with compound heterozygous *PEX16* mutations showed mildly increased very long chain fatty acids (VLCFAs) as previously described [19, 20]: C24:0/C22:0 1.15 [average 1.05, standard deviation (SD) 0.16], C25:0/C22:0 0.035 (average 0.024, SD 0.006), and C26:0/C22:0 0.038 (average 0.012, SD 0.005). Plasmalogen and phytanic acid were within normal range (data not shown). Brain MRI (Fig. 2) revealed cerebellar atrophy (both hemispheres and vermis) in eight patients (8/10, 80%), vermis atrophy/hypoplasia in two patients (2/10, 20%), and brainstem atrophy in one patient (1/10, 10%). Abnormal signal in the white matter was not observed in sibling patients 1A and 1B, but patient 1A showed decreased white matter volume (Fig. 2c). Calcification was recognized in the subcortical matter (patients 1A and 1B) and basal ganglia (patient 1B) (Fig. 2d). Molar tooth sign, which is a characteristic feature of Joubert syndrome, was observed in patient 2 with *C5orf42* mutations (Fig. 2f). Brain MRI in patient 3 with *C5orf42* mutations showed vermis hypoplasia, but no clear molar tooth sign as deepened interpeduncular fossa, secondary distortion and enlargement of the fourth ventricle, and horizontally oriented superior

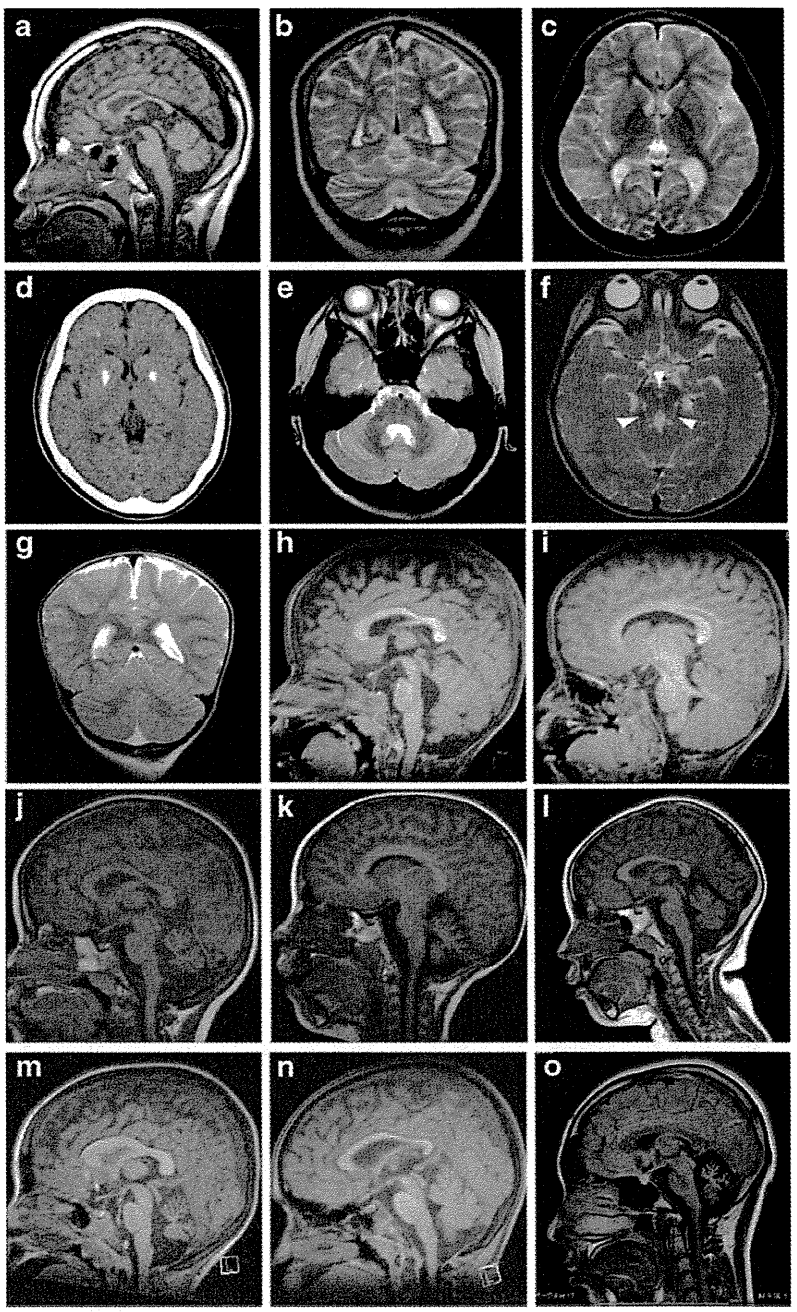

Fig. 2 **a**, **h**–**o** T1-weighted midline sagittal images, **b**, **g** T2-weighted coronal images, **c**, **e**, **f** T2-weighted axial images, **d** computed tomography images of the patients (**a**, **b**, **c**, patient 1A at 8 years of age; **d**, **e**, patient 1B at 12 years; **f**, patient 2 at 1 year and 8 months; **g**, **h**, **i** patient 3 at 1 year and 5 months; **j** patient 4 at 3 years; **k** patient 5 at 4 years; **l** patient 6 at 4 years; **m** patient 7 at 5 years; **n** patient 8 at 8 years; **o** patient 9 at 20 years). Vermis atrophy was observed in all patients (**b**, **e**, **f**, **g**, **j**–**o**) and very mild brain stem atrophy (especially in the basilar part of the pons) in patient 1A (**a**). In patient 1A, decreased volume but no abnormal signal in the white matter was observed (**c**). Calcification was observed in the subcortical white matter and basal ganglia of patient 1B (**d**). Patient 2 showed molar tooth sign (**f**, *arrowhead*), patient 3 showed vermis hypoplasia (**g**), but molar tooth sign was unclear as deepened interpeduncular fossa, secondary distortion and enlargement of the fourth ventricle, and horizontally oriented superior cerebellar peduncles were only mildly observed, with lack of thickened and elongated superior cerebellar peduncles (**h**, **i**)

cerebellar peduncles were only mildly observed, with lack of thickened and elongated superior cerebellar peduncles (Fig. 2g–i).

Discussion

In this report, the genetic basis of disorders showing cerebellar and/or vermis atrophy in childhood was successfully clarified in 9 of 23 families (39.1 %). Of note, mutations in seven distinct genes were identified, further supporting clinical and genetic heterogeneity of this condition. By family-based exome sequencing, we readily found three de novo mutations and six compound heterozygous mutations during a short period of time, demonstrating that family-based WES, when used with ethnically matched normal control exome data for prioritizing variants, is extremely powerful for dissecting genetic basis of neurological genetic disorders.

It is important to carefully address the relevance of identified mutations in respective cases by evaluating clinical information compared with previous reports and biochemical examination. Zellweger syndrome caused by *PEX16* mutations has been reported to show a very severe clinical course and white matter abnormalities [21]. Although patient 8 with *PEX16* mutations showed no white matter abnormalities and mild clinical features, Ebberink et al. recently reported patients with *PEX16* mutations, showing an atypical mild phenotype similar to our patient [19]. In addition, elevated VLCFAs levels, which are characteristic for *PEX16* mutations, were observed in our patient, supporting the notion that the identified *PEX16* mutations cause a relatively mild phenotype. Neuronal ceroid lipofuscinosis 2 caused by *TPP1* mutations is characterized by epilepsy, loss of vision, ataxia, and rapid progression [22]. Recently, Sun et al. showed that *TPP1* mutations can cause autosomal recessive SCAR7, which shows ataxia and low activity of tripeptidyl peptidase 1 [23]. Patient 6 with *TPP1* mutations showed epilepsy, ataxia, and low activity of tripeptidyl peptidase 1, suggesting that the phenotype was within the clinical spectrum caused by *TPP1* mutations.

De novo *CACNA1A* mutations were identified in patients 4 and 9, who showed no episodic ataxia or hemiplegia, a known phenotype caused by *CACNA1A* mutation [24]. However, cerebellar atrophy is a common feature of patients with *CACNA1A* mutations, and CAG repeat expansion in *CACNA1A* causes spinocerebellar ataxia type 6 (SCA6). In addition, the occurrence of de novo mutations has been estimated to be 7.6×10^{-9} and 2.2×10^{-8} per nucleotide in diploid embryos, suggesting that an average newborn is expected to acquire approximately 0.86 amino acid-altering mutations [25, 26]. Therefore, the chance coexistence of cerebellar atrophy and a de novo *CACNA1A* mutation in two independent patients is extremely rare, suggesting causal relationship between *CACNA1A* mutation and cerebellar atrophy. Haploinsufficiency of *ITPR1* was reported to cause adult-onset SCA15 associated with a slowly progressive pure type of cerebellar ataxia [27]. However, Huang et al. recently found that missense mutations in *ITPR1* caused infantile-onset SCA29 in two families, which is characterized by delayed motor development, cognitive delay, and cerebellar ataxia with cerebellar atrophy in a brain MRI [28]. The clinical features of our patient 7 with a de novo missense mutation in *ITPR1* is consistent with SCA29, confirming that *ITPR1* missense mutations can cause infantile-onset cerebellar atrophy.

We identified *C5orf42* mutations in patients 2 and 3 with vermis atrophy/hypoplasia. Molar tooth sign in brain MRI has been reported in patients with *C5orf42* mutations [29]. Although both patients showed hypotonia, developmental delay, mental retardation and oculomotor apraxia [30], characteristic molar tooth sign was only observed in patient 2. Therefore, retrospectively, patient 2 should be diagnosed with Joubert syndrome, but diagnosis of Joubert syndrome in patient 3 was challenging with no molar tooth sign. WES was able to provide correct genetic diagnosis in such atypical cases. Of note, in patients 1A and 1B with *FOLR1* mutations, folate deficiency can be improved with oral folinic acid administration [15, 16]. Therefore, genetic investigation by WES together with careful clinical evaluation will enhance correct diagnosis of patients, and may benefit their clinical management.

Acknowledgments We would like to thank all patients and their families for their participation in this study. We also thank Aya Narita and Nobuko Watanabe for technical assistance. This work was supported by the Ministry of Health, Labour, and Welfare of Japan; the Japan Society for the Promotion of Science (a Grant-in-Aid for Scientific Research (B) from (25293085, 25293235), a Grant-in-Aid for Scientific Research (A) (13313587)); the Takeda Science Foundation; the Japan Science and Technology Agency; the Strategic Research Program for Brain Sciences (11105137); and a Grant-in-Aid for Scientific Research on Innovative Areas (Transcription Cycle) from the Ministry of Education, Culture, Sports, Science, and Technology of Japan (12024421).

References

1. Poretti A, Wolf NI, Boltshauser E (2008) Differential diagnosis of cerebellar atrophy in childhood. Eur J Paediatr Neurol 12(3):155–167. doi:10.1016/j.ejpn.2007.07.010
2. Al-Maawali A, Blaser S, Yoon G (2012) Diagnostic approach to childhood-onset cerebellar atrophy: a 10-year retrospective study of 300 patients. J Child Neurol 27(9):1121–1132. doi:10.1177/0883073812448680
3. Schaefer AM, McFarland R, Blakely EL, He L, Whittaker RG, Taylor RW, Chinnery PF, Turnbull DM (2008) Prevalence of mitochondrial DNA disease in adults. Ann Neurol 63(1):35–39. doi:10.1002/ana.21217
4. Santorelli FM, Garavaglia B, Cardona F, Nardocci N, Bernardina BD, Sartori S, Suppiej A, Bertini E, Claps D, Battini R, Biancheri R, Filocamo M, Pezzini F, Simonati A (2013) Molecular epidemiology of childhood neuronal ceroid-lipofuscinosis in Italy. Orphanet J Rare Dis 8:19. doi:10.1186/1750-1172-8-19
5. Erichsen AK, Koht J, Stray-Pedersen A, Abdelnoor M, Tallaksen CM (2009) Prevalence of hereditary ataxia and spastic paraplegia in southeast Norway: a population-based study. Brain 132(Pt 6):1577–1588. doi:10.1093/brain/awp056
6. Matilla-Duenas A (2012) The ever expanding spinocerebellar ataxias. Editorial Cerebellum 11(4):821–827. doi:10.1007/s12311-012-0376-4
7. Valente EM, Brancati F, Boltshauser E, Dallapiccola B (2013) Clinical utility gene card for: Joubert syndrome—update 2013. Eur J Hum Genet. doi:10.1038/ejhg.2013.10
8. Vermeer S, van de Warrenburg BP, Willemsen MA, Cluitmans M, Scheffer H, Kremer BP, Knoers NV (2011) Autosomal recessive cerebellar ataxias: the current state of affairs. J Med Genet 48(10):651–659. doi:10.1136/jmedgenet-2011-100210
9. Bamshad MJ, Ng SB, Bigham AW, Tabor HK, Emond MJ, Nickerson DA, Shendure J (2011) Exome sequencing as a tool for Mendelian disease gene discovery. Nat Rev Genet 12(11):745–755. doi:10.1038/nrg3031
10. Vissers LE, de Ligt J, Gilissen C, Janssen I, Steehouwer M, de Vries P, van Lier B, Arts P, Wieskamp N, del Rosario M, van Bon BW, Hoischen A, de Vries BB, Brunner HG, Veltman JA (2010) A de

novo paradigm for mental retardation. Nat Genet 42(12):1109–1112. doi:10.1038/ng.712
11. de Ligt J, Willemsen MH, van Bon BW, Kleefstra T, Yntema HG, Kroes T, Vulto-van Silfhout AT, Koolen DA, de Vries P, Gilissen C, del Rosario M, Hoischen A, Scheffer H, de Vries BB, Brunner HG, Veltman JA, Vissers LE (2012) Diagnostic exome sequencing in persons with severe intellectual disability. N Engl J Med 367(20): 1921–1929. doi:10.1056/NEJMoa1206524
12. Saitsu H, Nishimura T, Muramatsu K, Kodera H, Kumada S, Sugai K, Kasai-Yoshida E, Sawaura N, Nishida H, Hoshino A, Ryujin F, Yoshioka S, Nishiyama K, Kondo Y, Tsurusaki Y, Nakashima M, Miyake N, Arakawa H, Kato M, Mizushima N, Matsumoto N (2013) *De novo* mutations in the autophagy gene *WDR45* cause static encephalopathy of childhood with neurodegeneration in adulthood. Nat Genet. doi:10.1038/ng.2562
13. Yamanaka H, Gatanaga H, Kosalaraksa P, Matsuoka-Aizawa S, Takahashi T, Kimura S, Oka S (2007) Novel mutation of human DNA polymerase gamma associated with mitochondrial toxicity induced by anti-HIV treatment. J Infect Dis 195(10):1419–1425. doi:10.1086/513872
14. Honsho M, Tamura S, Shimozawa N, Suzuki Y, Kondo N, Fujiki Y (1998) Mutation in PEX16 is causal in the peroxisome-deficient Zellweger syndrome of complementation group D. Am J Hum Genet 63(6):1622–1630. doi:10.1086/302161
15. Grapp M, Just IA, Linnankivi T, Wolf P, Lucke T, Hausler M, Gartner J, Steinfeld R (2012) Molecular characterization of folate receptor 1 mutations delineates cerebral folate transport deficiency. Brain 135(Pt 7):2022–2031. doi:10.1093/brain/aws122
16. Steinfeld R, Grapp M, Kraetzner R, Dreha-Kulaczewski S, Helms G, Dechent P, Wevers R, Grosso S, Gartner J (2009) Folate receptor alpha defect causes cerebral folate transport deficiency: a treatable neurodegenerative disorder associated with disturbed myelin metabolism. Am J Hum Genet 85(3):354–363. doi:10.1016/j.ajhg.2009.08.005
17. Lukacs Z, Santavuori P, Keil A, Steinfeld R, Kohlschutter A (2003) Rapid and simple assay for the determination of tripeptidyl peptidase and palmitoyl protein thioesterase activities in dried blood spots. Clin Chem 49(3):509–511
18. Sohar I, Lin L, Lobel P (2000) Enzyme-based diagnosis of classical late infantile neuronal ceroid lipofuscinosis: comparison of tripeptidyl peptidase I and pepstatin-insensitive protease assays. Clin Chem 46(7):1005–1008
19. Ebberink MS, Csanyi B, Chong WK, Denis S, Sharp P, Mooijer PA, Dekker CJ, Spooner C, Ngu LH, De Sousa C, Wanders RJ, Fietz MJ, Clayton PT, Waterham HR, Ferdinandusse S (2010) Identification of an unusual variant peroxisome biogenesis disorder caused by mutations in the *PEX16* gene. J Med Genet 47(9):608–615. doi:10.1136/jmg.2009.074302
20. Shimozawa N, Nagase T, Takemoto Y, Suzuki Y, Fujiki Y, Wanders RJ, Kondo N (2002) A novel aberrant splicing mutation of the *PEX16* gene in two patients with Zellweger syndrome. Biochem Biophys Res Commun 292(1):109–112
21. Steinberg SJ, Dodt G, Raymond GV, Braverman NE, Moser AB, Moser HW (2006) Peroxisome biogenesis disorders. Biochim Biophys Acta 1763(12):1733–1748. doi:10.1016/j.bbamcr.2006.09.010
22. Kousi M, Lehesjoki AE, Mole SE (2012) Update of the mutation spectrum and clinical correlations of over 360 mutations in eight genes that underlie the neuronal ceroid lipofuscinoses. Hum Mutat 33(1):42–63. doi:10.1002/humu.21624
23. Sun Y, Almomani R, Breedveld GJ, Santen GW, Aten E, Lefeber DJ, Hoff JI, Brusse E, Verheijen FW, Verdijk RM, Kriek M, Oostra B, Breuning MH, Losekoot M, den Dunnen JT, van de Warrenburg BP, Maat-Kievit AJ (2013) Autosomal recessive spinocerebellar ataxia 7 (SCAR7) is caused by variants in TPP1, the gene involved in classic late-infantile neuronal ceroid lipofuscinosis 2 disease (CLN2 disease). Hum Mutat 34(5):706–713. doi:10.1002/humu.22292
24. Haan J, Terwindt GM, van den Maagdenberg AM, Stam AH, Ferrari MD (2008) A review of the genetic relation between migraine and epilepsy. Cephalalgia 28(2):105–113. doi:10.1111/j.1468-2982.2007.01460.x
25. Roach JC, Glusman G, Smit AF, Huff CD, Hubley R, Shannon PT, Rowen L, Pant KP, Goodman N, Bamshad M, Shendure J, Drmanac R, Jorde LB, Hood L, Galas DJ (2010) Analysis of genetic inheritance in a family quartet by whole-genome sequencing. Science 328(5978):636–639. doi:10.1126/science.1186802
26. Lynch M (2010) Rate, molecular spectrum, and consequences of human mutation. Proc Natl Acad Sci U S A 107(3):961–968. doi:10.1073/pnas.0912629107
27. Durr A (2010) Autosomal dominant cerebellar ataxias: polyglutamine expansions and beyond. Lancet Neurol 9(9):885–894. doi:10.1016/s1474-4422(10)70183-6
28. Huang L, Chardon JW, Carter MT, Friend KL, Dudding TE, Schwartzentruber J, Zou R, Schofield PW, Douglas S, Bulman DE, Boycott KM (2012) Missense mutations in *ITPR1* cause autosomal dominant congenital nonprogressive spinocerebellar ataxia. Orphanet J Rare Dis 7:67. doi:10.1186/1750-1172-7-67
29. Srour M, Schwartzentruber J, Hamdan FF, Ospina LH, Patry L, Labuda D, Massicotte C, Dobrzeniecka S, Capo-Chichi JM, Papillon-Cavanagh S, Samuels ME, Boycott KM, Shevell MI, Laframboise R, Desilets V, Maranda B, Rouleau GA, Majewski J, Michaud JL (2012) Mutations in *C5ORF42* cause Joubert syndrome in the French Canadian population. Am J Hum Genet 90(4):693–700. doi:10.1016/j.ajhg.2012.02.011
30. Parisi MA, Doherty D, Chance PF, Glass IA (2007) Joubert syndrome (and related disorders) (OMIM 213300). Eur J Hum Genet 15(5):511–521. doi:10.1038/sj.ejhg.5201648

REPORT

Identification of *KLHL41* Mutations Implicates BTB-Kelch-Mediated Ubiquitination as an Alternate Pathway to Myofibrillar Disruption in Nemaline Myopathy

Vandana A. Gupta,[1] Gianina Ravenscroft,[2] Ranad Shaheen,[3] Emily J. Todd,[2] Lindsay C. Swanson,[1] Masaaki Shiina,[4] Kazuhiro Ogata,[4] Cynthia Hsu,[1] Nigel F. Clarke,[5] Basil T. Darras,[6] Michelle A. Farrar,[7] Amal Hashem,[3] Nicholas D. Manton,[8] Francesco Muntoni,[9] Kathryn N. North,[10] Sarah A. Sandaradura,[5] Ichizo Nishino,[11] Yukiko K. Hayashi,[11] Caroline A. Sewry,[9] Elizabeth M. Thompson,[12,13] Kyle S. Yau,[2] Catherine A. Brownstein,[1] Timothy W. Yu,[1] Richard J.N. Allcock,[14] Mark R. Davis,[15] Carina Wallgren-Pettersson,[16] Naomichi Matsumoto,[17] Fowzan S. Alkuraya,[3] Nigel G. Laing,[2] and Alan H. Beggs[1,*]

Nemaline myopathy (NM) is a rare congenital muscle disorder primarily affecting skeletal muscles that results in neonatal death in severe cases as a result of associated respiratory insufficiency. NM is thought to be a disease of sarcomeric thin filaments as six of eight known genes whose mutation can cause NM encode components of that structure, however, recent discoveries of mutations in non-thin filament genes has called this model in question. We performed whole-exome sequencing and have identified recessive small deletions and missense changes in the Kelch-like family member 41 gene (*KLHL41*) in four individuals from unrelated NM families. Sanger sequencing of 116 unrelated individuals with NM identified compound heterozygous changes in *KLHL41* in a fifth family. Mutations in *KLHL41* showed a clear phenotype-genotype correlation: Frameshift mutations resulted in severe phenotypes with neonatal death, whereas missense changes resulted in impaired motor function with survival into late childhood and/or early adulthood. Functional studies in zebrafish showed that loss of Klhl41 results in highly diminished motor function and myofibrillar disorganization, with nemaline body formation, the pathological hallmark of NM. These studies expand the genetic heterogeneity of NM and implicate a critical role of BTB-Kelch family members in maintenance of sarcomeric integrity in NM.

Nemaline myopathy (NM) is a rare congenital disorder primarily affecting skeletal muscle function. Clinically, NM is a heterogeneous group of myopathies of variable severity.[1,2] The "severe" congenital form of NM presents with reduced or absent spontaneous movements in utero leading to severe contractures or fractures at birth and respiratory insufficiency leading to early mortality. Individuals with the "intermediate" congenital form of NM have antigravity movement and independent respiration at delivery but exhibit delayed motor milestones and require ventilatory support later in life. The "typical" congenital form of NM usually presents in the neonatal period or first year of life with hypotonia, weakness, and feeding difficulties with less prominent respiratory involvement. In these cases, the disease is usually static or very slowly progressive, and many individuals remain ambulant for much of their lives.[3] The defining diagnostic feature of all forms of NM, irrespective of genetic mutation, is the presence of numerous red-staining rods with Gomori trichrome stain that appear as rod-shaped electron-dense structures termed "nemaline bodies" by electron microscopy.[4] These nemaline bodies are most frequently cytoplasmic; however, the presence of intranuclear rods has also been reported.[5]

NM is a genetically heterogeneous condition, and mutations in eight different genes have been identified that are associated with dominant and/or recessive forms of this disease.[6–13] Mutations in these genes cause about 75%–80% of NM cases, suggesting the involvement of additional unidentified genes in disease etiology.

[1]Division of Genetics and Genomics, The Manton Center for Orphan Disease Research, Boston Children's Hospital, Harvard Medical School, Boston, MA 02115, USA; [2]Western Australian Institute for Medical Research and the Centre for Medical Research, University of Western Australia, Nedlands, Western Australia 6009, Australia; [3]Developmental Genetics Unit, King Faisal Specialist Hospital and Research Center, Riyadh 11211, Saudi Arabia; [4]Department of Biochemistry, Yokohama City University, Graduate School of Medicine, 3-9 Fukuura, Kanazawa-ku, Yokohama 236-0004, Japan; [5]Institute for Neuroscience and Muscle Research, Children's Hospital at Westmead and Discipline of Paediatrics and Child Health, University of Sydney, Sydney 2145, Australia; [6]Department of Neurology, Boston Children's Hospital, Harvard Medical School, Boston, MA 02115, USA; [7]Department of Neurology, Sydney Children's Hospital, Randwick NSW 2032, Australia; [8]Department of Surgical Pathology, SA Pathology at the Women's and Children's Hospital, North Adelaide, South Australia 5006; [9]Dubowitz Neuromuscular Centre, Institute of Child Health and Great Ormond Street Hospital, London WC1N 1EH, UK; [10]Murdoch Childrens Research Institute, The Royal Children's Hospital, Parkville, Victoria 3052, Australia; [11]Department of Neuromuscular Research, National Institute of Neuroscience, National Center of Neurology and Psychiatry, Tokyo 187-8502, Japan; [12]Department of Paediatrics, University of Adelaide, Adelaide, South Australia 5000, Australia; [13]SA Clinical Genetics Service, SA Pathology at the Women's and Children's Hospital, North Adelaide, South Australia 5006, Australia; [14]Lotterywest State Biomedical Facility Genomics and School of Pathology and Laboratory Medicine, University of Western Australia, Perth, Western Australia 6000, Australia; [15]Department of Anatomical Pathology, Royal Perth Hospital, Perth, Western Australia 6000, Australia; [16]The Folkhälsan Institute of Genetics, Samfundet Folkhälsan, Biomedicum Helsinki, PB 63 (Haartmaninkatu 8), and Department of Medical Genetics, Haartman Institute, University of Helsinki, Helsinki 00014, Finland; [17]Department of Human Genetics, Yokohama City University, Graduate School of Medicine, 3-9 Fukuura, Kanazawa-ku, Yokohama 236-0004, Japan
*Correspondence: beggs@enders.tch.harvard.edu
http://dx.doi.org/10.1016/j.ajhg.2013.10.020.

Therefore, we performed whole-exome sequencing (WES) combined, when applicable, with autozygome analysis to identify mutations in novel genes that underlie the disease pathology in a cohort of individuals affected with NM with unknown genetic diagnosis. All subjects were enrolled following informed consent and research was conducted according to the protocols approved by the Institutional Review Boards of the respective institutions in which these individuals were recruited. Molecular screening was performed on genomic DNA isolated from blood samples following standard protocols.

We performed whole-exome or whole-genome sequencing on a cohort of 60 unrelated NM probands through Boston Children's Hospital Gene Partnership facility. Molecular screening was performed on genomic DNA isolated from blood samples with standard protocols. Whole-blood DNA was subjected to solution capture (SureSelect Human All Exon V4, Agilent Technologies) to generate barcoded whole-exome sequencing libraries. Libraries were sequenced on an Illumina HiSeq 2000, employing paired end reads (100 bp × 2) to a mean target coverage of 96.5% and a mean read depth of 71.6. Alignment, variant calling, and annotation were performed with a custom informatics pipeline employing BWA,[14] Picard, and ANNOVAR[15] focusing on rare (<3% in db SNP135, 1000 Genomes Project Database, and the [EVS] National Heart, Lung, and Blood Institute Exome Sequencing Project Exome Variant Server) protein affecting changes in known and novel human disease genes. Alternatively, probands for families 203 and 832 were sequenced to greater than 50× depth by Axeq Technologies on an Illumina HiSeq 2000 following Agilent SureSelect Exome enrichment with their standard Exome Sequencing service. Whole-exome sequencing identified homozygous mutations of *KLHL41* in two unrelated families, suggesting this gene to be a candidate for NM. All *KLHL41* mutations are numbered relative to the mRNA sequence NM_006063.2 (where position 1 is the first base of the initiating MET codon) and protein NP_006054.2. Family 1 is a nonconsanguineous family of Vietnamese origin. Proband 203-1 is a 16-year-old female with an intermediate form of NM with a high-arched palate, dysarthria, and scoliosis who has required ventilatory support since childhood. WES identified an apparently homozygous c.103T>C transition in exon 1 resulting in a p.Cys35Arg substitution in this individual (Figure 1A). This variant was present as heterozygous in the father and absent in the mother. Copy number analysis in the affected region showed a heterozygous deletion in the mother and the proband, c.(?_-77)_(*602_?)del. Therefore, individual 203-1 is compound heterozygous for a deletion involving a portion of *KLHL41* and a KLHL41 p.Cys35Arg missense change. The second proband (832-1), who is adopted of Russian origin, is ambulant at age 12 and exhibits the typical congenital form of NM. WES identified a homozygous deletion of one base and an insertion of four bases c.459delinsACTC in the proband resulting in a single amino acid insertion, p.Ser153_Ala154insLeu in the protein (Figure 1A).

Whole-exome sequencing in probands with severe NM in Australian and Saudi Arabian cohorts resulted in identification of *KLHL41* mutations in two further families. The first (6462) is a consanguineous family of Persian origin from Afghanistan with one child (D12-203) affected with severe NM and four unaffected children (see Figure S1 available online). Homozygosity mapping was performed on the proband with the Illumina HumanCytoSNP-12 array, and the only known NM loci found within homozygous regions were *CFL2* (MIM 601443) and *NEB* (MIM 161650); however, both were excluded following Sanger sequencing, as was *ACTA1* (MIM 102610), which is the most common cause of simplex NM cases. WES of DNA from proband D12-203 was performed at the Lotterywest Sate Biomedical Facility Genomics Node, Royal Perth Hospital, Western Australia.[13] WES identified 453 heterozygous or homozygous variants. Application of the homozygosity data to the list of candidates reduced this to seven candidate variants. Two of these seven candidate variants were in skeletal-muscle-specific genes and of these the most likely candidate was a homozygous deletion within *KLHL41* (chr2: 170382132–170382139; c.1748_1755delAAGGAAAT, p.Lys583Thrfs*7) (Figure 1A). The deletion was confirmed by Sanger sequencing. Both parents and two unaffected siblings were heterozygous for the deletion, and two further unaffected siblings were homozygous for the normal allele.

Family 12DG1177, from a Saudi Arabian cohort is consanguineous (Figure S1). The male proband (12DG1177-1) was a newborn with severe hypotonia, dislocation of hips and knees, and facial dysmorphism in the form of micrognathia and cleft palate. There was a positive family history of two previous sibs who died of unknown causes soon after birth, as well as three healthy living sibs. The proband died of cardiorespiratory arrest shortly after intubation at less than 24 hr of age. Exome capture was performed with TruSeq Exome Enrichment kit (Illumina) as described earlier.[16] Only novel coding and splicing homozygous variants within the autozygome of the affected individual were considered. After filtering, 8,653 homozygous, coding, or splice variants were present, and autozygosity mapping, dbSNP, and analysis of 240 control Saudi exomes finally led to the identification of 18 candidate variants. The only truncating change was a single base deletion in *KLHL41* (c.641delA). This deletion was present in the coding region of exon 1 of *KLHL41* resulting in the frameshift change p.Asn214Thrfs*14 (Figure 1A).

Subsequent screening for *KLHL41* mutations in 116 individuals affected with severe, intermediate, or typical congenital forms of NM in the Boston and Australian NM Cohorts by Sanger sequencing identified a further family (D10-236) with compound heterozygous mutation (c.581_583delAAG, p.Glu194del and c.1238C>T, p.Ser413Leu) in proband. This individual is of Chinese

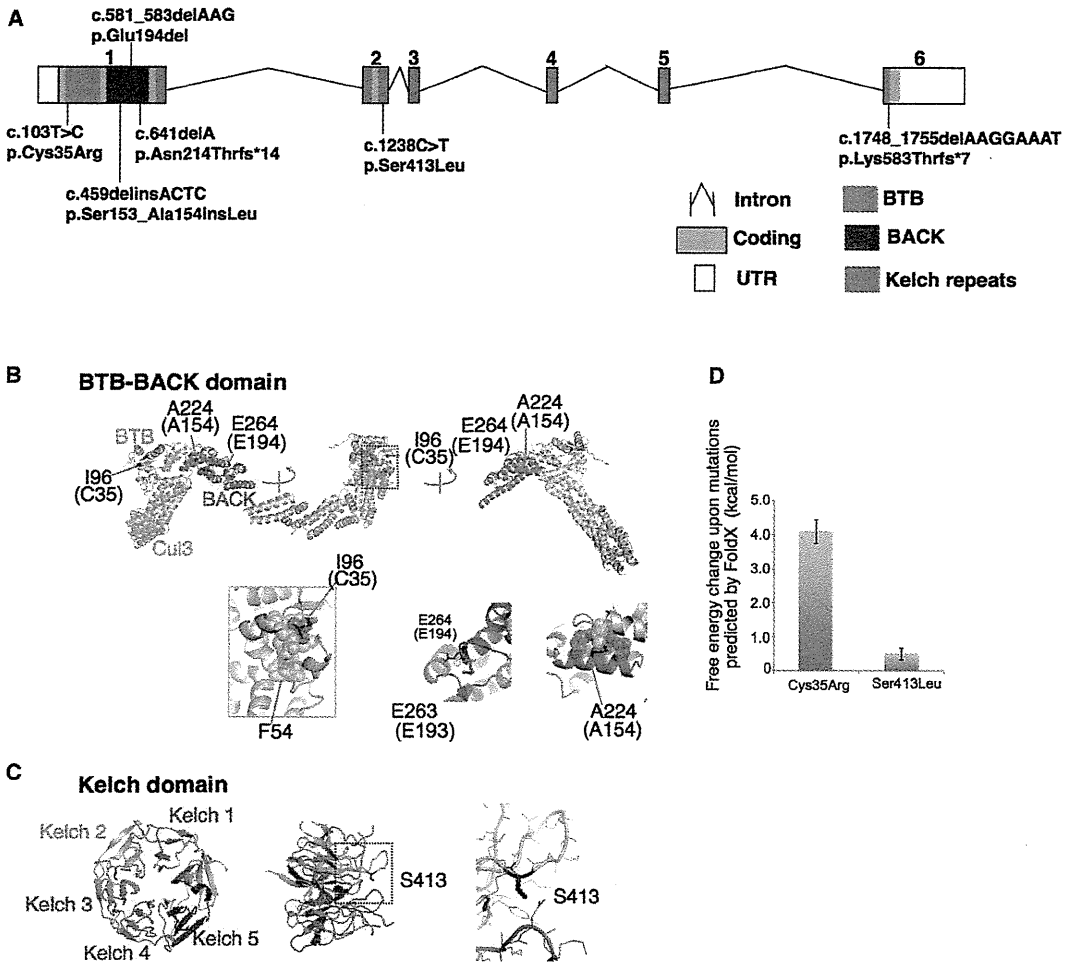

Figure 1. Overview of Mutations in *KLHL41* and Their Effect on Protein Structure

(A) Schematic representation of mutations in *KLHL41*. Boxes represent exons 1–6. Conserved domains of KLHL41 are indicated as follows: BTB (blue), BACK (red), and Kelch repeats (green). The BTB and BACK domains are encoded by exon 1 and the five Kelch repeats are encoded by exons 1–6.

(B and C) Crystal structures of the BTB-BACK domain of human Kelch-like protein (KLHL11) in complex with CUL3 (Protein Data Bank code 4AP2) (B) and the Kelch domain of rat KLHL41 (PDB code 2WOZ) (C). α helices, β strands, and loops are drawn as ribbons, arrows, and threads, respectively. The squared areas correspond to the close-up views in the insets. In (B), the BTB and BACK domains are colored pink and green, respectively, whereas CUL3 is colored yellow, except that Ile96, Ala224, and Glu264 (Cys35, Ala154, and Glu194 in human KLHL41, respectively) are colored red. The side chains of these residues and Glu263 (Glu193 in human KLHL41) are shown as sticks with the indications of amino acid numbers for human KLHL11 and those for human KLHL41 in parentheses. Side chains involved in hydrophobic cores around Ile96 and Ala224 are drawn in van der Waal's representation. In (C), the Kelch domain is color-coded to indicate each Kelch repeat, except that Ser413 is colored red. The side chain of Ser413 is shown as sticks. Molecular structures are drawn with PyMOL.

(D) Predicted free energy changes upon the substitutions of KLHL41 with FoldX software.

origin and exhibited the typical congenital form of NM. The detailed clinical features of affected individuals with mutations identified in *KLHL41* are presented in Table 1.

Overall, WES and Sanger sequencing resulted in identification of seven different mutations in Kelch-like family member 41 (*KLHL41*), previously known as *KBTBD10*, sarcosin, or *KRP1*, in affected NM individuals from five unrelated families (Figure 1A). Muscle histology was typical for NM: biopsies from probands of three different families (D12-203, 832-1, and 10-236) exhibited abnormal Gomori trichrome staining with presence of sarcoplasmic rods that varied from numerous small rods to fewer large rods in multiple myofibers (Figure 2A). No intranuclear rods or cores were seen. The missense changes identified in *KLHL41* are predicted to be pathogenic by polyphen, SIFT and pMUT and the mutated amino-acid residues are conserved in all representative species during evolution (Figure S2). The neighboring areas surrounding the sites of insertion or deletion are also relatively conserved, suggesting a structural or functional requirement for the altered amino acid residues (Figure S2). Sequencing of family members revealed that *KLHL41*

Table1. Clinical Manifestations in Affected Individuals Harboring *KLHL41* Mutations

Proband ID	cDNA Change	Amino Acid Change	Clinical Category	Sex	Nationality	Pregnancy and Delivery	Alive at Age/Mobility/ Age at Death	Associated Features
203-1	c.103T>C c.(?_-77)_(*602_?)del	p.Cys35Arg Heterozygous p.0? Heterozygous	Intermediate	F	Vietnamese	Normal	16 yrs, uses wheelchair (ambulant 24–36 mo)	Ventilated 24 hr from 5 yrs. High-arched palate, dysarthria Scoliosis
832-1	c.459delinsACTC	p.Ser153_Ala154insLeu Homozygous	Other forms (grade of severity: mild)	M	Russian	No data	12 yrs, ambulant	Distal weakness > proximal distal contractures
D10-236	c.581_583delAAG c.1238C>T	p.Glu194del Heterozygous p.Ser413Leu Heterozygous	Typical form	M	Chinese	Normal - h 40	5 yrs, ambulant	VSD, finger contractures, focal renal echogenicity
D12-203	c.1748_1755del AAGGAAAT,	p.Lys583Thrfs*7 Homozygous	Fetal akinesia sequence	M	Persian	Polyhydramnios, breech presentation, emergency Cesarean section - h 31+2	Died at 3 mo (active support discontinued)	Arthrogryposis, macrocephaly, hypospadias No antigravity movements at birth
12DG1177	c.641delA	p.Asn214Thrfs*14 Homozygous	Severe form Fetal akinesia sequence	M	Saudi Arabian	Fetal movements weak, breech presentation	Died during 1st day of life	Dislocation of hips and knees, cleft palate, micrognathia, narrow chest

mutations showed a segregation pattern compatible with a recessive mode of inheritance in all families (Figure S1). Severe phenotypes associated with genetic null mutations and intermediate or typical congenital forms with mutations that should results in presence of residual protein, suggests a phenotype-genotype correlation in individuals affected with *KLHL41* mutations.

KLHL41 belongs to the family of BTB-Kelch domain-containing proteins.[17–20] Mutations in two other members of this family, *KBTBD13* (MIM 613727), and most recently *KLHL40* (MIM 615430), have been associated with a clinically distinct form of congenital myopathy exhibiting nemaline bodies, as well as multiminicores and severe NM, respectively.[12,13] To evaluate the impacts of the *KLHL41* mutations on the protein structure, we mapped them onto the crystal structures of the BTB-BACK domain of human KLHL11 in complex with human CUL3, a subunit of E3 ubiquitin ligases, (PDB code 4AP2)[21] and the Kelch domain of rat KLHL41 (PDB code 2WOZ),[22] analogous to those domains of human KLHL41. The Cys35 side chain is involved in a hydrophobic core of the BTB domain, which makes van der Waals contacts with Phe54 of Cul3 (Figure 1B). The p.Cys35Arg substitution present in affected individual 203-1 would likely destabilize the hydrophobic core and thereby impair the interaction with Cul3. This was supported by the FoldX result, in which free energy change upon the p.Cys35Arg substitution was predicted to be over 4 kcal/mol, which can be interpreted as considerable destabilization of a protein structure (Figure 1D; Figure S3).[23] In proband 832-1, a Leu residue is inserted between the amino acid positions 153 and 154 in the center of a helix, in which several residues are involved in a hydrophobic core of the BACK domain (Figure 1B). This amino acid insertion is likely to destabilize the BACK domain fold. In proband D10-236, the p.Ser413Leu substitution was mapped to a loop region, which is located near the substrate-binding region of the Kelch repeat 2 (Figure 1C; Figure S1B). A FoldX calculation predicted that the p.Ser413Leu substitution would have minimal effect on stability of the Kelch domain (Figure 1D). The effect of Glu194 deletion at the N-terminal end of an α helix can be compensated by the presence of Glu193 located in the loop (Figure 1B). Nonetheless, it cannot be excluded that the p.Ser413Leu and p.Glu194del changes alter the protein solubility or aggregate tendency and/or impair substrate binding. The conserved nature of the mutated KLHL41 domains, as well as the potential role of the mutations in disrupting those structural domains, supports the likely pathogenicity of these mutations.

The localization of KLHL41 in skeletal muscles was investigated by immunofluorescence of mouse FDB cultured myofibers and human skeletal muscle cryosections. Immunofluorescence with two different antibodies against N-terminal (Sigma, AV38732) and C-terminal parts of human KLHL41 (Abcam, ab66605) was performed, and z stacks were acquired by confocal microscopy as described

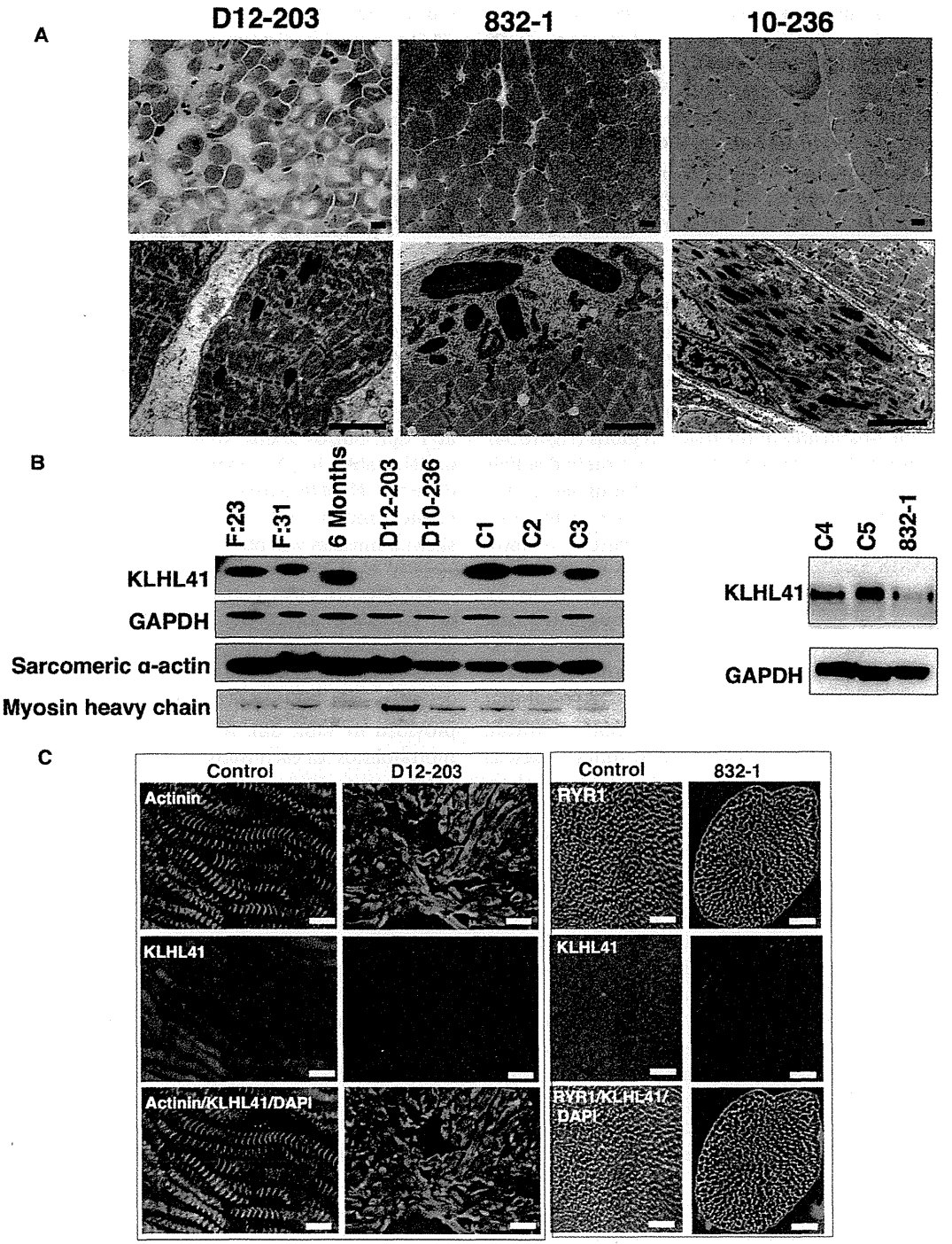

Figure 2. Muscle Pathology and Expression of KLHL41 Levels and Localization in Muscle of Affected Individuals
(A) Light microscopy of Gomori trichrome stained skeletal muscle from affected individuals with *KLHL41* mutations show cytoplasmic nemaline bodies (top panel). Electron microscopy of affected muscles reveals rods of variable frequency and size and severe myofibrillar disarray (bottom panels). (Scale bars represent 2 μm). Affected individuals' IDs are indicated at top.
(B) Immunoblotting analysis of KLHL41 levels in affected and unaffected muscles. A decrease in protein levels was observed in individuals with *KLHL41* mutations in comparison to normal control muscles. Immunoblotting with sarcomeric actin or Coomassie staining of myosin heavy chain showed no abnormal accumulation of sarcomeric proteins in affected muscles. Immunostaining for GAPDH was used for loading controls. Lanes: F:23, 23 week control fetus; F:30, 31 week control fetus; 6-month-old control baby, C1–C5 are normal age-matched control muscles.
(C) Immunofluorescence for KLHL41 in control and affected individual muscle biopsies showed highly reduced levels of KLHL41 in longitudinally oriented (left) or transverse sections (right) of skeletal muscles from affected individuals. Scale bars represent 50 μm.

previously.[24] Immunofluorescence with both antibodies resulted in similar staining patterns; however, due to lower background staining, the C-terminal antibody was used for further studies. Costaining with sarcomeric markers in longitudinal planes showed that KLHL41 staining predominated over the I-bands of the sarcomere and at perinuclear regions in human biopsies (Figure 2C) and murine cultured myofibers (Figure S4). Analysis of transverse sections of myofibers from control human biopsies revealed KLHL41 staining in a ring pattern around the myofibrils, generally colocalizing with ryanodine receptors (RYR1), which are a marker of the sarcoplasmic reticulum (Figure S5). Together, these observations suggest that KLHL41 localizes over (but not within) I bands, likely in association with the terminal cisternae of the sarcomplasmic reticulum (SR) and longitudinal vesicles of the SR present in the I-band area at the triadic regions (Figure S4). Colocalization studies with the ER marker protein disulfide isomerase (PDI) in myofibers and skeletal muscles further confirmed the localization of KLHL41 in SR-ER membranes (Figures S4). This overall localization pattern is most consistent with localization to the endoplasmic reticulum (ER) around myonuclei and to microdomains of the SR with ER characteristics.[25] Previous studies suggested that the closely related NM protein, KLHL40, localized at A-bands,[13] but double label immunofluorescence studies of both longitudinal and transverse sections here reveal that it appears colocalized with RYR1, around but not within the myofibrils in cultured myofibers and human skeletal muscles in a pattern overlapping, but not identical to, that of KLHL41 (Figures S4 and S5). These associations of proteins whose defects cause NM with the ER/SR contrasts with previously known NM proteins, all of which are sarcomeric thin filament components, with the exception of KBTBD13 whose localization is not well known.

In mouse tissues, immunoblotting detected KLHL41 in skeletal muscle and diaphragm (Figure S6). In cultured murine C2C12 cells, KLHL41 levels increased during differentiation to myotubes (Figure S6). Immunoblotting of affected skeletal muscle extracts revealed greatly reduced levels of KLHL41 in individuals with *KLHL41* mutations (Figure 2B) and immunofluorescence microscopy of affected individuals' skeletal muscles also showed that KLHL41 levels were greatly reduced in their myofibers (Figure 2C).

Cell culture studies have shown that KLHL41 interacts with nebulin, N-RAP (Nebulin-related anchoring protein), and actin in skeletal muscle and promotes the assembly of myofibrils.[26] KLHL41 regulates skeletal muscle differentiation as overexpression or knockdown inhibited C2C12 myoblast differentiation.[27] Knockdown of *Klhl41* in cultured cardiomyocytes resulted in sarcomeric disorganization with thickening of Z-lines as seen in NM.[28] However, the exact functions of KLHL41 in disease pathology are unknown. Recent studies have identified mutations in two other closely related family members *KBTBD13* and *KLHL40* as causes of NM suggesting the crucial requirement for several Kelch family proteins in skeletal muscle function.[12,13] To investigate the functional role of KLHL41 in vertebrate skeletal muscle development, we employed zebrafish as a model system. Zebrafish have two duplicated orthologs (*klhl41a* and *klhl41b*) that share ~80% similarity with *KLHL41*. Zebrafish whole-mount in situ hybridization was performed to study the spatio-temporal expression of these genes during zebrafish development as described previously.[29] Specifically, RNA probes specific for each Klhl41 gene were generated by amplification of the 3′ UTRs from a cDNA library of 2 day postfertilization (dpf) zebrafish embryos, followed by in vitro transcription to generate digoxigenin-labeled antisense transcripts (primer sequences are provided in Table S1). Whole-mount in situ hybridization showed ubiquitous expression of *klhl41a* during early development at 1 dpf, but by 2 dpf, *klhl41a* transcripts were virtually undetectable in the major axial skeletal muscles. In contract, *klhl41b* expression was predominantly seen in striated muscles, and strong expression in heart and skeletal muscles was observed throughout zebrafish development to at least 5 dpf (Figure 3A).

The effect of KLHL41 deficiency in zebrafish was studied by knocking down the Klhl41 genes with antisense morpholinos. Two independent morpholinos targeting an exon-intron spice site and translational start site were designed for both genes (morpholino sequences are provided in Table S2). As initial experiments with both morpholinos for each transcript resulted in similar phenotypes, we performed the remainder of our studies with the splice-site morpholinos (7 ng). *klhl41a* morphants exhibited leaner bodies, smaller eyes, and pericardial edema as seen in other myopathy models (n = 65–110) (Figure 3B).[30,31] Examination of 3 dpf morphants with polarized light showed reduced birefringence in axial skeletal muscles suggesting disorganized skeletal muscle structure (Figure 3B; Figure S7). Knockdown of *klhl41b* resulted in reduced birefringence without any other significant abnormalities (n = 82–132). Targeting both *klhl41a* and *klhl41b* (7 ng each) resulted in curved bodies with a 30% reduction in size along with small eyes and pericardial edema (n = 89–103), compared to fish injected with control morpholino (14ng). *klhl41a* morphant fish die by 3 dpf while *klhl41b* morphants typically did not survive past 5 dpf. Knockdown of both genes was lethal by 3 dpf. Double knockdown fish exhibited severely disorganized muscle (measured by reduced birefringence) compared to controls and either of the single knockdowns. RT-PCR and immunoblotting confirmed the knockdown of *klhl41a* and *klhl41b* transcripts and a reduction in protein levels (Figures 3C and 3D). Overexpression of human *KLHL41* mRNA in the double morphants resulted in a significant increase in the number of surviving fish with normal birefringence suggesting the specificity of morpholino injections and demonstrating the ability of this single evolutionary ortholog to complement both zebrafish genes (Figure 3E). Behavioral characterization of 3

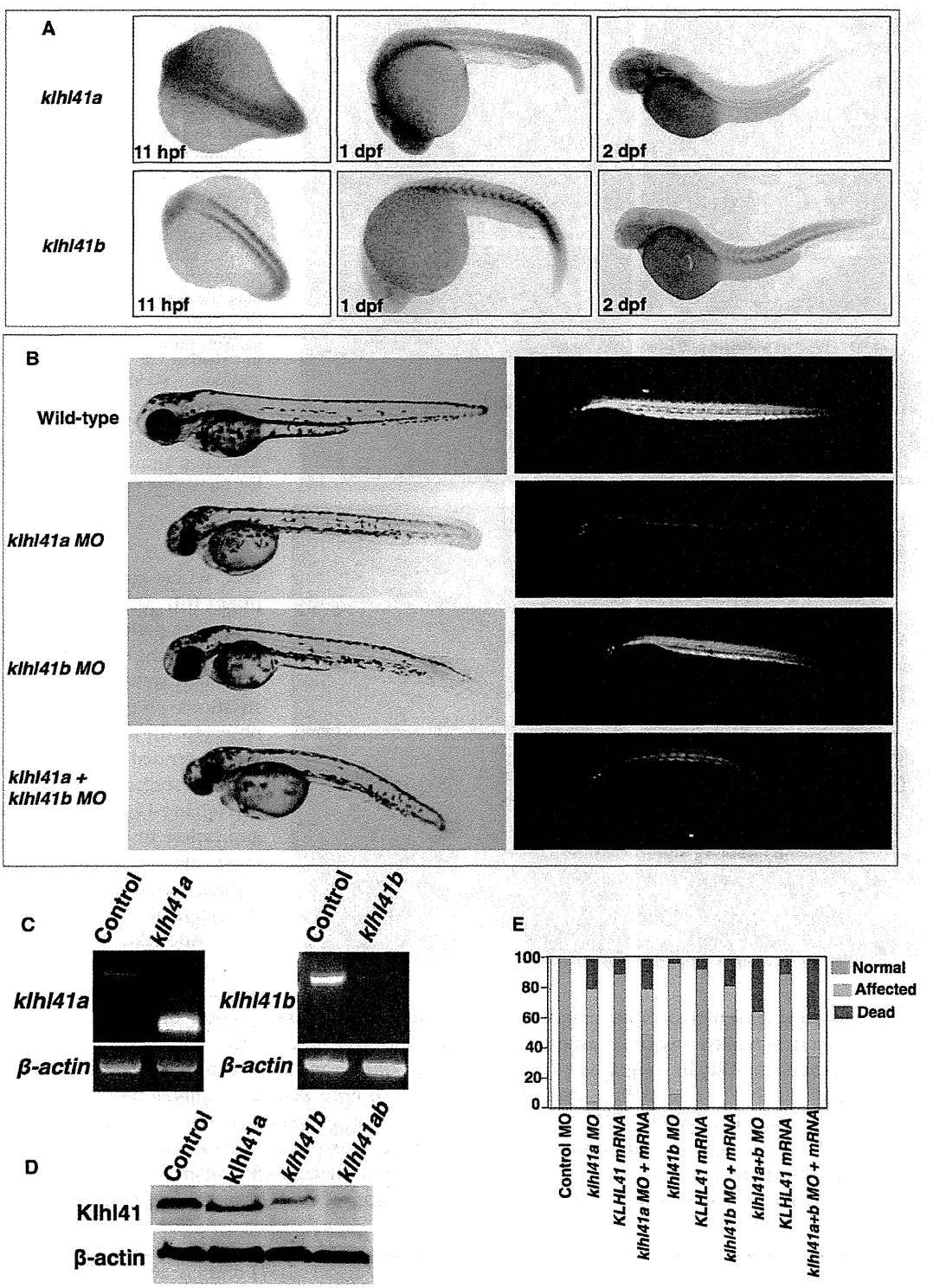

Figure 3. Characterization and Knockdown of Zebrafish Orthologs of *KLHL41*

(A) In situ hybridization of the zebrafish Klhl41 genes shows early expression during myogenesis in developing somites (11 hr after fertilization). *Klhl41a* is expressed in brain, eyes, and muscle at 1 dpf. Later in development expression is largely restricted to brain and heart (2 dpf), although low levels of expression in axial slow skeletal myofibers cannot be excluded due to limited sensitivity of the assay. *Klhl41b* expression is localized to skeletal muscle and heart at all developmental stages (1–2 dpf).

(B) Knockdown of Klhl41 genes in zebrafish using antisense morpholinos results in myopathic changes. Live microscopy of zebrafish embryos at 3 dpf reveals leaner and smaller bodies in comparison to wild-type (WT) fish. Under polarized microscopy, zebrafish embryos

(legend continued on next page)

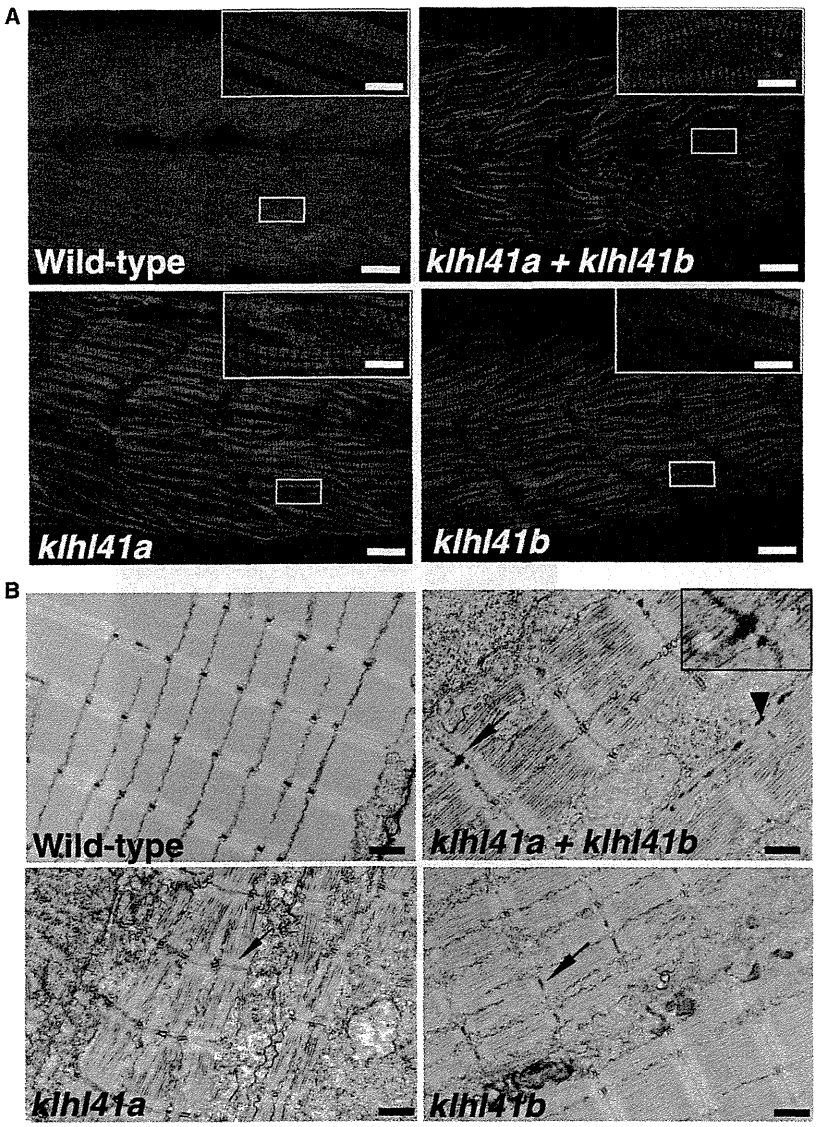

Figure 4. Loss of *klhl41* Function in Zebrafish Recapitulates the Disease Pathology of Human Nemaline Myopathies
(A) Whole-mount staining of 3 dpf zebrafish embryos with phalloidin showed extensive myofibrillar disarray of myofibers in *klhl41* morphant fish (scale bar represents 2 μm). Three dpf embryos fixed in 4% paraformaldehyde were incubated with phalloidin (Invitrogen, A12380, 1:40) overnight at 4°C. Skeletal muscles of klhl41-deficient embryos were smaller and exhibited an overall reduction of myofibrillar organization (inset, high magnification).
(B) Electron microscopy of klhl41-deficient skeletal muscle revealed thickened Z-lines in *klhl41a* or *klhl41b* morphants. In addition, skeletal muscle of double knockdown fish contained electron dense bodies, reminiscent of nascent nemaline rods (arrowhead, nemaline bodies like structures; arrow, thickened Z-lines) (scale bar represents 1 μm).

dpf morphant fish, knocked down for either or both Klhl41 genes, using the touch-evoked response assay showed significantly diminished motility in comparison to control fish (WT fish: 5.74 ± 0.98 cm/0.1 s; *klhl41a*: 1.32 ± 0.61 cm/0.1 s; *klhl41b*: 2.00 ± 0.49 cm/0.1 s; *klhl41ab*: 0.73 ± 0.39 cm/0.1 s), suggesting a significant degree of overall muscle weakness (Movies S1, S2, S3, and S4).[32] To visualize abnormalities in sarcomeric architecture, whole-mount staining of morphant fish and control zebrafish embryos was performed with phalloidin to stain the actin-thin filaments. Although well-organized myofibrillar striations (i.e., sarcomeres) were observed, the myofibrils in *klhl41* morphants tended to be thinner and were highly disorganized relative to control fish (Figure 4A). The myofibrilar disorganization in *klhl41* morphants was also evident by evaluation of ultrathin toluidine blue sections of control and morphant fish (Figure S7). The main diagnostic feature of NM is the presence of nemaline rods with or without Z-line streaming in skeletal muscle. Ultrastructural examination of zebrafish skeletal muscle by electron microscopy showed Z-line thickening in both *klhl41a* and *klhl41b* morphant fish (Figure 4B). Knockdown of both *klhla* and *klhl41b* resulted in the presence of numerous electron-dense structures, reminiscent of small or nascent nemaline bodies, in addition to Z-line thickening (Figure 4B). Given the differences in temporal expression of *klhl41a* (early embryogenesis) and *klhl41b*

exhibit a reduction in birefringence in morphant fish, quantified in ImageJ as described (WT controls: 100% ± 5.9% *klhl41a*: 23% ± 3.0%; *klhl41b*: 31% ± 8.2%; *klhl41ab*: 16% ± 4.2%). Double knockdown fish show a more severe skeletal muscle phenotype than single morphants.
(C) RT-PCR analysis showed knockdown of normal transcripts in the morphant fish.
(D) Immunoblot analysis showed reduction in Klhl41 levels in *klhl41a*, *klhl41b*, and *klhl41ab* fish. Klhl41 antibody recognizes both klhl41a and klhl41b and therefore show immunoreactibility to the other gene in the single morphants that is highly reduced in double morphants.
(E) Overexpression of human *KLHL41* mRNA restores the skeletal muscle phenotypes of *klhl41a/b* single and double morphants suggesting morpholino specificity. The mRNA concentration used to rescue were as follows: *klhl41a* (50 pg), *klhl41b* (75 pg), *klhl41a+b* (60 pg of each).

(maintained later in development), and the high degree of structural and functional conservation (both are rescued by the single human transcript), it is likely that increased severity of *klhl41a* morphants is due to this being the predominant embryonic isoform at the early stages targeted by morpholino injections.

Extensive skeletal muscle disorganization associated with sarcomeric abnormalities in morphant fish points toward a function of KLHL41 in skeletal muscle development and maintenance. Mutations affecting the closely related BTB-Kelch family member KLHL40 have recently also been reported to cause nemaline myopathy.[13] While *KLHL40* mutations resulted in a severe clinical presentation in most of the affected individuals, KLHL41 abnormalities are associated with a spectrum of phenotypes from severe with neonatal death, to survival into late childhood. However, no significant differences were seen in skeletal muscle pathology. KLHL40 contains a putative nuclear localization sequence (NLS) and is expressed throughout muscle differentiation, whereas KLHL41 lacks NLS and is expressed in late differentiation (Figure S8).[13] KLHL41 and many other BTB domain-containing Kelch family members are known to interact with Cul3 ubiquitin ligase to form functional ubiquitination complexes with proteins targeted for degradation.[21,33] KLHL41, which has been shown to interact with nebulin,[34] is now the third BTB-Kelch family member to be identified as a cause of NM when mutated. We hypothesize that improper surveillance and degradation of aberrant thin-filament proteins might explain the convergent pathological and clinical phenotypes associated with mutations of thin filament and BTB-Kelch family member genes in NM.

Supplemental Data

Supplemental Data include eight figures, two tables, and four movies and can be found with this article online at http://www.cell.com/AJHG/home.

Acknowledgments

We are grateful to the many NM affected individuals and their families, and to their treating physicians, for their participation in this research. Whole-exome sequencing was made possible through the generous support and assistance of David Margulies and the entire staff of The Gene Partnership Project at Boston Children's Hospital. We would like to thank Pankaj Agrawal and Wen-Hann Tan for many helpful discussions during the course of this work. We are thankful to Louise Trakimas of the electron microscope facility at Harvard Medical School for excellent help with zebrafish histology, and the Genotyping and Sequencing Core Facilities at KFSHRC for their technical help. V.A.G. is supported by K01 AR062601 from the National Institute of Arthritis and Musculoskeletal and Skin Diseases of National Institute of Health. This work was also supported by the Muscular Dystrophy Association of USA (MDA201302), National Institutes of Health grant from the National Institute of Arthritis and Musculoskeletal and Skin Diseases R01 AR044345, the AUism Charitable Foundation, and A Foundation Building Strength (to A.H.B.); National Health and Medical Research Council of Australia Early Career Researcher Fellowship #1035955 (to G.R.); Research Fellowship APP1002147 and Project Grant APP1022707(to N.G.L.); the Association Française contre les Myopathies (#15734), Dubai-Harvard Foundation for Medical Research Collaborative Research Grant (to F.S.A.); a UWA Collaborative Research Award (G.R.); and the Great Ormond Street Hospital Children's Charity (to F.M.). E.J.T. and K.S.Y. are supported by University of Western Australia Postgraduate Awards. DNA sequencing was performed by the Boston Children's Hospital Genomics Program Molecular Genetics Core, and confocal microscopy was performed at Boston Children's Hospital Intellectual and Developmental Disability Research Center Imaging Core, both supported by National Institutes of Health grant P30 HD18655. The funders had no role in study design, data collection and analysis, decision to publish, or preparation of the manuscript.

Received: August 9, 2013
Revised: October 15, 2013
Accepted: October 22, 2013
Published: November 21, 2013

Web Resources

The URLs for data presented herein are as follows:

1000 Genomes, http://browser.1000genomes.org
dbSNP, http://www.ncbi.nlm.nih.gov/projects/SNP/
NHLBI Exome Sequencing Project (ESP) Exome Variant Server, http://evs.gs.washington.edu/EVS/
Online Mendelian Inheritance in Man (OMIM), http://www.omim.org/
Picard, http://picard.sourceforge.net/
Pymol, http://www.pymol.org

References

1. Wallgren-Pettersson, C., Sewry, C.A., Nowak, K.J., and Laing, N.G. (2011). Nemaline myopathies. Semin. Pediatr. Neurol. *18*, 230–238.
2. Ryan, M.M., Schnell, C., Strickland, C.D., Shield, L.K., Morgan, G., Iannaccone, S.T., Laing, N.G., Beggs, A.H., and North, K.N. (2001). Nemaline myopathy: a clinical study of 143 cases. Ann. Neurol. *50*, 312–320.
3. Wallgren-Pettersson, C. (2002). Nemaline and myotubular myopathies. Semin. Pediatr. Neurol. *9*, 132–144.
4. Sewry, C.A. (2008). Pathological defects in congenital myopathies. J. Muscle Res. Cell Motil. *29*, 231–238.
5. Hutchinson, D.O., Charlton, A., Laing, N.G., Ilkovski, B., and North, K.N. (2006). Autosomal dominant nemaline myopathy with intranuclear rods due to mutation of the skeletal muscle ACTA1 gene: clinical and pathological variability within a kindred. Neuromuscul. Disord. *16*, 113–121.
6. Pelin, K., Hilpelä, P., Donner, K., Sewry, C., Akkari, P.A., Wilton, S.D., Wattanasirichaigoon, D., Bang, M.L., Centner, T., Hanefeld, F., et al. (1999). Mutations in the nebulin gene associated with autosomal recessive nemaline myopathy. Proc. Natl. Acad. Sci. USA *96*, 2305–2310.
7. Nowak, K.J., Wattanasirichaigoon, D., Goebel, H.H., Wilce, M., Pelin, K., Donner, K., Jacob, R.L., Hübner, C., Oexle, K., Anderson, J.R., et al. (1999). Mutations in the skeletal muscle

alpha-actin gene in patients with actin myopathy and nemaline myopathy. Nat. Genet. *23*, 208–212.
8. Laing, N.G., Wilton, S.D., Akkari, P.A., Dorosz, S., Boundy, K., Kneebone, C., Blumbergs, P., White, S., Watkins, H., Love, D.R., et al. (1995). A mutation in the alpha tropomyosin gene TPM3 associated with autosomal dominant nemaline myopathy. Nat. Genet. *9*, 75–79.
9. Tajsharghi, H., Ohlsson, M., Lindberg, C., and Oldfors, A. (2007). Congenital myopathy with nemaline rods and cap structures caused by a mutation in the beta-tropomyosin gene (TPM2). Arch. Neurol. *64*, 1334–1338.
10. Agrawal, P.B., Greenleaf, R.S., Tomczak, K.K., Lehtokari, V.L., Wallgren-Pettersson, C., Wallefeld, W., Laing, N.G., Darras, B.T., Maciver, S.K., Dormitzer, P.R., and Beggs, A.H. (2007). Nemaline myopathy with minicores caused by mutation of the CFL2 gene encoding the skeletal muscle actin-binding protein, cofilin-2. Am. J. Hum. Genet. *80*, 162–167.
11. Johnston, J.J., Kelley, R.I., Crawford, T.O., Morton, D.H., Agarwala, R., Koch, T., Schäffer, A.A., Francomano, C.A., and Biesecker, L.G. (2000). A novel nemaline myopathy in the Amish caused by a mutation in troponin T1. Am. J. Hum. Genet. *67*, 814–821.
12. Sambuughin, N., Yau, K.S., Olivé, M., Duff, R.M., Bayarsaikhan, M., Lu, S., Gonzalez-Mera, L., Sivadorai, P., Nowak, K.J., Ravenscroft, G., et al. (2010). Dominant mutations in KBTBD13, a member of the BTB/Kelch family, cause nemaline myopathy with cores. Am. J. Hum. Genet. *87*, 842–847.
13. Ravenscroft, G., Miyatake, S., Lehtokari, V.L., Todd, E.J., Vornanen, P., Yau, K.S., Hayashi, Y.K., Miyake, N., Tsurusaki, Y., Doi, H., et al. (2013). Mutations in KLHL40 are a frequent cause of severe autosomal-recessive nemaline myopathy. Am. J. Hum. Genet. *93*, 6–18.
14. Li, H., and Durbin, R. (2009). Fast and accurate short read alignment with Burrows-Wheeler transform. Bioinformatics *25*, 1754–1760.
15. Wang, K., Li, M., and Hakonarson, H. (2010). ANNOVAR: functional annotation of genetic variants from high-throughput sequencing data. Nucleic Acids Res. *38*, e164.
16. Alkuraya, F.S. (2012). Discovery of rare homozygous mutations from studies of consanguineous pedigrees. Curr Protoc Hum Genet. *Chapter 6*, Unit 6, 12.
17. Adams, J., Kelso, R., and Cooley, L. (2000). The kelch repeat superfamily of proteins: propellers of cell function. Trends Cell Biol. *10*, 17–24.
18. Dhanoa, B.S., Cogliati, T., Satish, A.G., Bruford, E.A., and Friedman, J.S. (2013). Update on the Kelch-like (KLHL) gene family. Hum. Genomics *7*, 13.
19. du Puy, L., Beqqali, A., van Tol, H.T., Monshouwer-Kloots, J., Passier, R., Haagsman, H.P., and Roelen, B.A. (2012). Sarcosin (Krp1) in skeletal muscle differentiation: gene expression profiling and knockdown experiments. Int. J. Dev. Biol. *56*, 301–309.
20. Gray, C.H., McGarry, L.C., Spence, H.J., Riboldi-Tunnicliffe, A., and Ozanne, B.W. (2009). Novel beta-propeller of the BTB-Kelch protein Krp1 provides a binding site for Lasp-1 that is necessary for pseudopodial extension. J. Biol. Chem. *284*, 30498–30507.
21. Canning, P., Cooper, C.D., Krojer, T., Murray, J.W., Pike, A.C., Chaikuad, A., Keates, T., Thangaratnarajah, C., Hojzan, V., Marsden, B.D., et al. (2013). Structural basis for Cul3 protein assembly with the BTB-Kelch family of E3 ubiquitin ligases. J. Biol. Chem. *288*, 7803–7814.
22. Spence, H.J., Johnston, I., Ewart, K., Buchanan, S.J., Fitzgerald, U., and Ozanne, B.W. (2000). Krp1, a novel kelch related protein that is involved in pseudopod elongation in transformed cells. Oncogene *19*, 1266–1276.
23. Guerois, R., Nielsen, J.E., and Serrano, L. (2002). Predicting changes in the stability of proteins and protein complexes: a study of more than 1000 mutations. J. Mol. Biol. *320*, 369–387.
24. Lawlor, M.W., Alexander, M.S., Viola, M.G., Meng, H., Joubert, R., Gupta, V., Motohashi, N., Manfready, R.A., Hsu, C.P., Huang, P., et al. (2012). Myotubularin-deficient myoblasts display increased apoptosis, delayed proliferation, and poor cell engraftment. Am. J. Pathol. *181*, 961–968.
25. Kaisto, T., and Metsikkö, K. (2003). Distribution of the endoplasmic reticulum and its relationship with the sarcoplasmic reticulum in skeletal myofibers. Exp. Cell Res. *289*, 47–57.
26. Lu, S., Carroll, S.L., Herrera, A.H., Ozanne, B., and Horowits, R. (2003). New N-RAP-binding partners alpha-actinin, filamin and Krp1 detected by yeast two-hybrid screening: implications for myofibril assembly. J. Cell Sci. *116*, 2169–2178.
27. Paxton, C.W., Cosgrove, R.A., Drozd, A.C., Wiggins, E.L., Woodhouse, S., Watson, R.A., Spence, H.J., Ozanne, B.W., and Pell, J.M. (2011). BTB-Kelch protein Krp1 regulates proliferation and differentiation of myoblasts. Am. J. Physiol. Cell Physiol. *300*, C1345–C1355.
28. Greenberg, C.C., Connelly, P.S., Daniels, M.P., and Horowits, R. (2008). Krp1 (Sarcosin) promotes lateral fusion of myofibril assembly intermediates in cultured mouse cardiomyocytes. Exp. Cell Res. *314*, 1177–1191.
29. Gupta, V., Discenza, M., Guyon, J.R., Kunkel, L.M., and Beggs, A.H. (2012). α-Actinin-2 deficiency results in sarcomeric defects in zebrafish that cannot be rescued by α-actinin-3 revealing functional differences between sarcomeric isoforms. FASEB J. *26*, 1892–1908.
30. Dowling, J.J., Vreede, A.P., Low, S.E., Gibbs, E.M., Kuwada, J.Y., Bonnemann, C.G., and Feldman, E.L. (2009). Loss of myotubularin function results in T-tubule disorganization in zebrafish and human myotubular myopathy. PLoS Genet. *5*, e1000372.
31. Gupta, V.A., Kawahara, G., Myers, J.A., Chen, A.T., Hall, T.E., Manzini, M.C., Currie, P.D., Zhou, Y., Zon, L.I., Kunkel, L.M., and Beggs, A.H. (2012). A splice site mutation in laminin-α2 results in a severe muscular dystrophy and growth abnormalities in zebrafish. PLoS ONE *7*, e43794.
32. Smith, L.S., Beggs, A.H., and Gupta, V.A. (2013). Analysis of skeletal muscle defects in larval zebrafish by birefringence and touch-evoke escape response assays. J. Vis. Exp. *82*, e50925. http://dx.doi.org/10.3791/50925.
33. Zhang, D.D., Lo, S.C., Sun, Z., Habib, G.M., Lieberman, M.W., and Hannink, M. (2005). Ubiquitination of Keap1, a BTB-Kelch substrate adaptor protein for Cul3, targets Keap1 for degradation by a proteasome-independent pathway. J. Biol. Chem. *280*, 30091–30099.
34. Spence, H.J., McGarry, L., Chew, C.S., Carragher, N.O., Scott-Carragher, L.A., Yuan, Z., Croft, D.R., Olson, M.F., Frame, M., and Ozanne, B.W. (2006). AP-1 differentially expressed proteins Krp1 and fibronectin cooperatively enhance Rho-ROCK-independent mesenchymal invasion by altering the function, localization, and activity of nondifferentially expressed proteins. Mol. Cell. Biol. *26*, 1480–1495.

Journal of Human Genetics (2013) 58, 822–824

www.nature.com/jhg

SHORT COMMUNICATION

Novel *FIG4* mutations in Yunis–Varon syndrome

Junya Nakajima[1,2], Nobuhiko Okamoto[3], Jun Shiraishi[4], Gen Nishimura[5], Mitsuko Nakashima[1], Yoshinori Tsurusaki[1], Hirotomo Saitsu[1], Hisashi Kawashima[2], Naomichi Matsumoto[1] and Noriko Miyake[1]

Yunis–Varon syndrome (YVS, MIM 216340) is a rare autosomal recessive disorder characterized by skeletal abnormalities and severe neurological impairment with vacuolation of the central nervous system, skeletal muscles and cartilages. Very recently, mutations of the *FIG4* (FIG4 homolog, SAC1 lipid phosphatase domain containing (*Saccharomyces cerevisiae*)) gene, which encodes a 5′-phosphoinositide phosphatase essential for endosome/lysosome function have been identified as the cause for YVS. Interestingly, *FIG4* mutations were previously reported to be responsible for other neurodegenerative diseases such as autosomal recessive Charcot–Marie–Tooth disease type 4J and autosomal dominant amyotrophic lateral sclerosis/primary lateral sclerosis. We analyzed a YVS patient using whole-exome sequencing, and identified novel biallelic *FIG4* mutations: c.1750 + 1delG and c.2284_2285delCT (p.S762Wfs*3). These two mutations were mutations supposed to have null function. To our knowledge, this is the second report of *FIG4* mutations in YVS and our result supports the idea that biallelic null mutations of *FIG4* cause YVS in human.
Journal of Human Genetics (2013) **58,** 822–824; doi:10.1038/jhg.2013.104; published online 3 October 2013

Keywords: biallelic mutation; *FIG4*; whole-exome sequencing; Yunis–Varon syndrome

Yunis–Varon syndrome (YVS, MIM_216340) is a rare autosomal recessive disorder characterized by skeletal abnormalities (cleidocranial dysostosis, bilateral absence of thumbs and halluces distal aphalangia and pelvic bone dysplasia) and severe neurological impairment.[1] Recently, mutations of *FIG4* (FIG4 homolog, SAC1 lipid phosphatase domain containing (*Saccharomyces cerevisiae*); NM_014845.5) were identified as the genetic cause for YVS.[2] *FIG4* encodes FIG4 protein (also known as SAC3) which is a 5′-phosphoinositide phosphatase essential for endosome/lysosome function.[3] FIG4 binds with Vac14/ArPIKfyve and Fab1/PIKfyve to form a functional complex on early endosomal membranes known as PIKfyve–ArPIKfyve–Sac3 complex.[3] The PIKfyve–ArPIKfyve–Sac3 complex mediates the conversion of endosomal phosphatidylinositol 3-phosphate (PI3P) to phosphatidylinositol 3,5-biphosphate ($PI(3,5)P_2$), and this conversion is essential for protein sorting, trafficking late endosomes to lysosomal degradation compartment and regulating some other endolysosome/lysosome functions essential for degradation such as ion channel activation and endolysosome fusion/fission.[4] Impairment of FIG4 causes a reduction of $PI(3,5)P_2$, which results in the malfunction of the endosome/endolysosome/lysosome. Therefore, the accumulation of undegraded materials in these compartments leads to dilatation.[3]

FIG4 abnormalities were previously reported to be the causative for autosomal recessive Charcot–Marie–Tooth disease type 4J (CMT4J, MIM#611228) and autosomal dominant amyotrophic lateral sclerosis (ALS, MIM#105400)/primary lateral sclerosis (PLS, MIM#611637).[2,5–7] Vacuolated endolysosomes are found in the perinuclear regions of peripheral neurons of *Fig4*-null mice and CMT4J patients.[3] In YVS patients, vacuolation was observed in skeletal muscles, fibroblasts and the central nervous system including cerebral cortex, the basal ganglia, cerebellar olives and medullary olives.[8–10]

The patient was a 2-year-old girl at the time of genetic consultation. She was the second daughter of a nonconsanguineous pair of 32-year-old woman and a 25-year-old man. Both her parents and her sister were healthy. Fetal echogram revealed intrauterine growth retardation. She was born at 40 weeks of gestation, with Apgar scores of 2 and 1 at 1 and 5 min, respectively. Her birth weight was 3306 g (+0.6 SD), body length 52 cm (+1.5 SD) and head circumference 33 cm (−0.3 SD). Because of neonatal asphyxia, she was transferred to neonatal intensive care unit and supported by mechanical ventilation. Lower anal atresia was found and colostomy was performed. Tube feeding was necessary because of poor feeding activity. Tracheostomy was placed at 8 months of age because of severe respiratory impairment. She presented with characteristic face (protruding forehead, wide fontanels, temporal narrowing, hypertelorism, blepharophimosis, inverted epicanthus, flat nasal bridge, bilateral low set ears, short philtrum, high-arched palate, down-turned mouth,

[1]Department of Human Genetics, Yokohama City University Graduate School of Medicine, Yokohama, Japan; [2]Department of Pediatrics, Tokyo Medical University, Shinjuku, Japan; [3]Department of Medical Genetics, Osaka Medical Center and Research Institute for Maternal and Child Health, Izumi, Japan; [4]Department of Neonatal Medicine, Osaka Medical Center and Research Institute for Maternal and Child Health, Izumi, Japan and [5]Department of Radiology, Tokyo Metropolitan Children's Medical Center, Fuchu, Japan.
Correspondence: Dr N Miyake or Dr N Matsumoto, Department of Human Genetics, Yokohama City University Graduate School of Medicine, Fukuura 3-9, Kanazawa-ku, Yokohama 236-0004, Japan.
E-mail: nmiyake@yokohama-cu.ac.jp or naomat@yokohama-cu.ac.jp
Received 27 June 2013; revised 31 August 2013; accepted 2 September 2013; published online 3 October 2013